Additional Mechanisms for Providing Clear Stabilization (Consistency) Diagrams

A.W. Phillips, R.J. Allemang
Structural Dynamics Research Laboratory
Department of Mechanical Engineering
University of Cincinnati
Cincinnati, OH 45221-0072 USA
Email: Allyn.Phillips@UC.EDU

ABSTRACT

Recently, there has been renewed interest in methods and techniques of reducing the confusion and uncertainty associated with the morass of spurious, computational poles that result from the traditional over-determined equation set in modal parameter estimation processes. In this paper, several additional mechanisms for providing a clear stabilization, or consistency, diagram are presented. Among these, the effect of frequency scaling and symbol characteristics based upon other modal information are used as a mechanism for identifying and eliminating computational poles.

Nomenclature

$N_i =$ Number of inputs.
$N_o =$ Number of outputs.
$N =$ Number of modal frequencies.
$\omega_i =$ Frequency (rad/sec).
$\lambda_r =$ Complex modal frequency
$s_i =$ Generalized frequency variable.
$m =$ Model order for denominator polynomial.
$n =$ Model order for numerator polynomial.
$n_u =$ Model order residual polynomial (Lower).
$n_l =$ Model order residual polynomial (Upper).
$||v|| =$ Norm of vector v.
$A_{pqr} =$ Residue: output DOF p, input DOF q, mode r.
$[R_k] =$ Residual polynomial coefficient.
$[\alpha] =$ Numerator polynomial matrix coefficient.
$[\beta] =$ Denominator polynomial matrix coefficient.
$[I] =$ Identity matrix.
$[H(\omega_i)] =$ FRF matrix ($N_o \times N_i$)).
$X(\omega_i) =$ Response function vector ($N_o \times 1$)).
$F(\omega_i) =$ Input function vector ($N_i \times 1$)).
$MPC =$ Mean Phase Coefficient.

1. Introduction

For the last thirty years, modal parameter estimation based upon experimental data, primarily frequency response functions (FRFs), has utilized some form of error chart and/or stabilization diagram to visualize and assist in the determination of the correct modal frequencies [1-3]. The conceptual basis of the stabilization diagram is that distinct and unique modal frequencies can be identified by comparing the roots of a characteristic polynomial when the model order of the characteristic polynomial is increased. If the roots are consistent as the model order is increased, these roots are identified as modal frequencies. If the roots are inconsistent, these roots are associated with noise on the data and are discarded. Since there is generally much more FRF data available than is needed to solve for the number of modal parameters of interest, the characteristic polynomial is normally estimated in a least squares sense and can be reformulated from the measured FRFs for each model order.

In most implementations, the **stabilization diagram** or **consistency diagram** is presented as a two dimensional plot with frequency on the abscissa and characteristic polynomial model order on the ordinate. A plot of the summed magnitude of all of the FRFs, or a plot of one of the mode indicator functions (complex mode indicator function (CMIF) or multivariate mode indicator function (MvMIF)), is

placed in the background for reference. For each model order, symbols are plotted along the frequency axis wherever a root of the characteristic polynomial has been estimated. Historically, the characteristic polynomial had scalar coefficients (single reference data) so the roots are complex-valued and have both frequency and damping information. The original symbols were used to indicate, in increasing importance, Level 1: a pole was found, Level 2: a pole was found with an associated complex conjugate, Level 3: Level 2 plus the damping was realistic (negative real part of pole), Level 4: Level 3 plus a damped natural frequency (imaginary part of pole) consistency within a specified percentage (normally 1 percent) and Level 5: Level 4 plus a damping consistency with a specified percentage (normally 5 percent). As multiple reference parameter estimation was developed, this led to matrix coefficient, characteristic polynomial equations which created further evaluation criteria, Level 6: Level 5 plus a vector consistency within a specified modal assurance criterion (MAC) value (normally 0.95). Since the vector that is associated with the matrix coefficient, characteristic polynomial may be different sizes (function of N_i or N_o), a variation of Level 6 involves an additional solution for the vector at the largest dimension of N_i or N_o so that a more statistically significant comparison of vectors can be utilized. Finally, numerical conditioning can be evaluated for each solution and if the numerical conditioning is approaching a limit based upon the accuracy of the data or the numerical limitations of the computer algorithm or word size, Level 7 can be added to indicate a possible numerical problem. In general, all of the specified values that indicate consistency at each level can be user defined and are referred to as the stability or consistency tolerances.

This much information generates a consistency diagram, for a simple circular plate structure, that looks like Figure 1. With all of the symbols presented, the consistency diagram for even this simple structure can be very complicated.

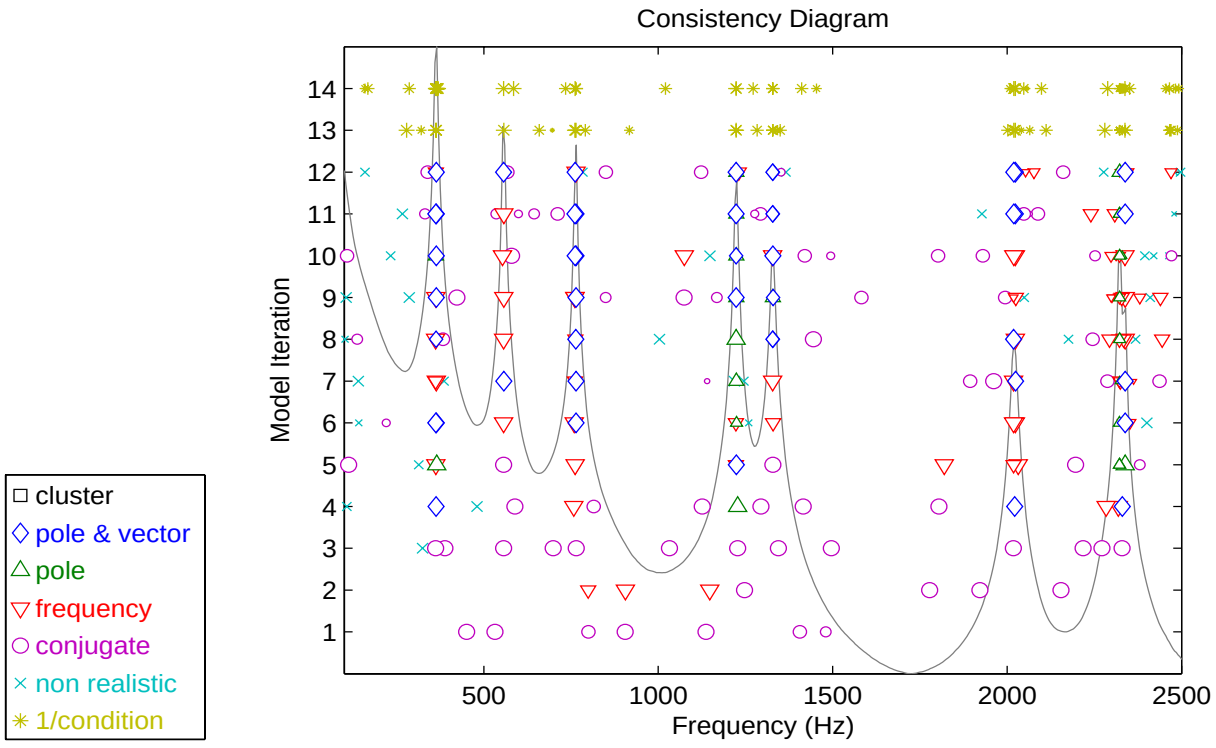

Figure 1. Typical Consistency Diagram

For this reason, in today's commercial implementations, many of the symbols are no longer utilized or can be optionally presented or suppressed. This, together with the adjustment of the consistency percentage (tolerance) levels for frequency, damping and vector, gives the first approach to a clear stabilization diagram as is shown in Figure 2. Note that the grey areas of the legend for this diagram indicate that those symbols have been suppressed.

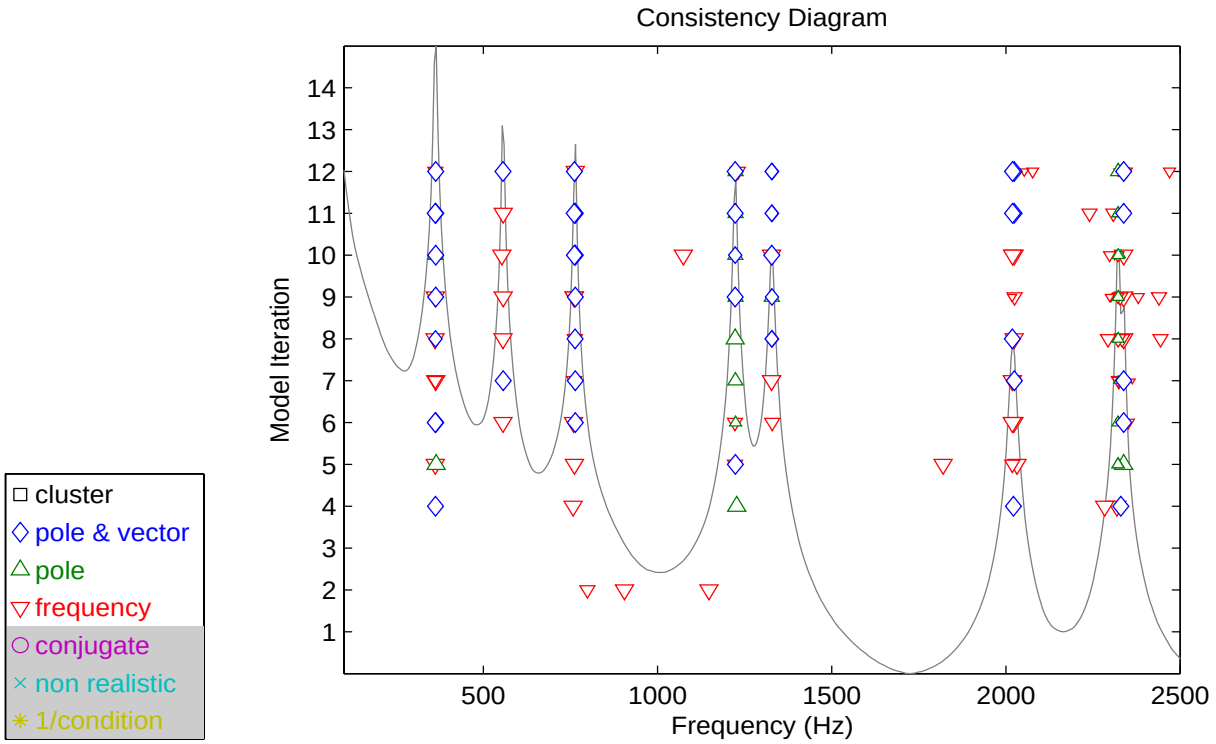

Figure 2. Typical Consistency Diagram with Some Indicators Suppressed

The term, **stabilization diagram**, was initially chosen to describe this diagram and is still used by most commercial implementations. However, the estimation of the roots at each model order is inherrently stable and the diagram is describing the consistency of the roots of a characteristic polynomial from one solution to the previous. For this reason, the diagram is also commonly referred to as a **consistency diagram**. Note that in the original development, the consistency diagram was based upon succesive increase in the model order of the characteristic polynomial. Therefore, each horizontal line of symbols were derived from an increase in the model order by one. In this paper, this concept will be extended to allow any sequence of changes in the ordinate direction.

2. Background

All modern, commercial algorithms for estimating modal parameters from experimental input-output data can be developed or explained in terms of polynomial based models. For this reason, with minor implementation differences, all of these algorithms can take advantage of the consistency diagram as an aid in identifying the correct modal frequencies from the large number of poles that are found. This section quickly overviews the development of the polynomial models for both time and frequency domain so that the model order variation options, that are involved in the consistency diagram, can be discussed. This background is detailed more fully in several references [2-6]. The algorithms that commonly use an implementation of the consistency diagram for identifying modal parameters are summarized in Table 1.

2.1 Polynomial Modal Identification Models

Rather than using a physically based mathematical model, the common characteristics of different modal parameter estimation algorithms can be more readily identified by using a matrix coefficient polynomial model. One way of understanding the basis of this model can be developed from the polynomial model used historically for the frequency response function. Note the nomenclature in the following equations regarding measured frequency ω_i versus generalized frequency s_i. Measured input and response data are always functions of measured frequency but the generalized frequency variable used in the model may be altered to improve the numerical conditioning as is done with most frequency domain methods (normalized frequency) and specifically with the polyreference least squares complex frequency (PLSCF)

method (complex Z transform of frequency). The commercial implementation of the PLSCF method is known as PolyMAX ®.

$$H_{pq}(s_i) = \frac{X_p(s_i)}{F_q(s_i)} = \frac{\beta_n (s_i)^n + \beta_{n-1} (s_i)^{n-1} + \cdots + \beta_1 (s_i)^1 + \beta_0 (s_i)^0}{\alpha_m (s_i)^m + \alpha_{m-1} (s_i)^{m-1} + \cdots + \alpha_1 (s_i)^1 + \alpha_0 (s_i)^0} \tag{1}$$

This can be rewritten in linear form by clearing the fraction, rearranging and collecting the unknown α and β terms:

$$\sum_{k=0}^{m} \alpha_k (s_i)^k X_p(s_i) = \sum_{k=0}^{n} \beta_k (s_i)^k F_q(s_i) \tag{2}$$

This model can be generalized to represent the general multiple input, multiple output case as follows:

$$\sum_{k=0}^{m} \left[[\alpha_k] (s_i)^k \right] \{X(s_i)\} = \sum_{k=0}^{n} \left[[\beta_k] (s_i)^k \right] \{F(s_i)\} \tag{3}$$

Note that the size of the coefficient matrices $[\alpha_k]$ will normally be $N_i \times N_i$ or $N_o \times N_o$ and the size of the coefficient matrices $[\beta_k]$ will normally be $N_i \times N_o$ or $N_o \times N_i$ when the equations are developed from experimental data.

Rather than developing the basic model in terms of force and response information, the models can be stated in terms of power spectra or frequency response information. First, post multiply both sides of the equation by $\{F\}^H$:

$$\sum_{k=0}^{m} \left[[\alpha_k] (s_i)^k \right] \{X(s_i)\} \{F(s_i)\}^H = \sum_{k=0}^{n} \left[[\beta_k] (s_i)^k \right] \{F(s_i)\} \{F(s_i)\}^H \tag{4}$$

Now recognize that the product of $\{X(s_i)\} \{F(s_i)\}^H$ is the output-input cross spectra matrix ($[G_{xf}(s_i)]$) for one ensemble and $\{F(s_i)\} \{F(s_i)\}^H$ is the input-input cross spectra matrix ($[G_{ff}(s_i)]$) for one ensemble. With a number of ensembles (averages), these matrices are the common matrices used to estimate the FRFs in a MIMO case. This yields the following cross spectra model:

$$\sum_{k=0}^{m} \left[[\alpha_k] (s_i)^k \right] \left[G_{xf}(s_i) \right] = \sum_{k=0}^{n} \left[[\beta_k] (s_i)^k \right] \left[G_{ff}(s_i) \right] \tag{5}$$

The previous cross spectra model can be reformulated to utilize frequency response function (FRF) data by post multiplying both sides of the equation by $[G_{ff}(s_i)]^{-1}$:

$$\sum_{k=0}^{m} \left[[\alpha_k] (s_i)^k \right] \left[G_{xf}(s_i) \right] \left[G_{ff}(s_i) \right]^{-1} = \sum_{k=0}^{n} \left[[\beta_k] (s_i)^k \right] \left[G_{ff}(s_i) \right] \left[G_{ff}(s_i) \right]^{-1} \tag{6}$$

Therefore, the multiple input, multiple output (MIMO) FRF model is:

$$\sum_{k=0}^{m} \left[[\alpha_k] (s_i)^k \right] \left[H(s_i) \right] = \sum_{k=0}^{n} \left[[\beta_k] (s_i)^k \right] [I] \tag{7}$$

Equation (7) is evaluated at many frequencies (ω_i) until all data are utilized or a sufficient overdetermination factor is achieved. Note that both positive and negative frequencies are required in order to accurately estimate conjugate modal frequencies. This allows for the coefficients of a matrix coefficient, characteristic polynomial to be identified for a given model order m. The roots of this polynomial can be used to find the modal parameters.

Paralleling the development of Equations (1) through (7), a time domain model representing the relationship between a single response degree of freedom and a single input degree of freedom can be stated as follows:

$$\sum_{k=0}^{m} \alpha_k \; x(t_{i+k}) = \sum_{k=0}^{n} \beta_k \; f(t_{i+k}) \tag{8}$$

For the general multiple input, multiple output case:

$$\sum_{k=0}^{m} [\alpha_k] \; \{x(t_{i+k})\} = \sum_{k=0}^{n} [\beta_k] \; \{f(t_{i+k})\} \tag{9}$$

If the discussion is limited to the use of free decay or impulse response function data, the previous time domain equations can be simplified by noting that the forcing function can be assumed to be zero for all time greater than zero. If this is the case, the $[\beta_k]$ coefficients can be eliminated from the equations.

$$\sum_{k=0}^{m} [\alpha_k] \left[h(t_{i+k}) \right] = 0 \tag{10}$$

Additional equations can be developed by repeating Equation (10) at different time shifts into the data (t_i) until all data are utilized or a sufficient overdetermination factor is achieved. Note that at least one time shift is required in order to accurately estimate conjugate modal frequencies. This allows for the coefficients of the matrix coefficient, characteristic polynomial to be identified for a given model order m. The roots of this polynomial can be used to find the modal parameters.

The models represented by Equation (7) and Equation (10) are referred to as a **Unified Matrix Polynomial Approach (UMPA)**, models. Both models yield a matrix coefficient, characteristic polynomial (the $[\alpha]$ polynomial in these models). Equation (10) corresponds to a time domain AutoRegressive-Moving-Average (ARMA(m,n)) model, or more properly an AutoRegressive with eXogenous inputs (ARX(m,n)) model, that is developed from a set of discrete time equations. Since both the frequency and time domain models are based upon functionally similar matrix coefficient, characteristic polynomials, the UMPA terminology will be used for models in both domains.

In light of the above discussion, it is now apparent that most of the modal parameter estimation processes available could have been developed by starting from a general matrix polynomial formulation that is justifiable based upon the underlying matrix differential equation. The general matrix polynomial formulation yields essentially the same form of matrix coefficient, characteristic polynomial equation, for both time and frequency domain data.

For the frequency domain data case, this yields:

$$\left| \; [\alpha_m] \; s^m + [\alpha_{m-1}] \; s^{m-1} + [\alpha_{m-2}] \; s^{m-2} + \ldots\ldots\ldots + [\alpha_0] \; \right| = 0 \tag{11}$$

where:

$$s_r = \lambda_r \qquad \lambda_r = \sigma_r + j \; \omega_r \tag{12}$$

For the time domain data case, this yields:

$$\left| [\alpha_m]\, z^m + [\alpha_{m-1}]\, z^{m-1} + [\alpha_{m-2}]\, z^{m-2} + \ldots\ldots\ldots + [\alpha_0] \right| = 0 \tag{13}$$

where:

$$z_r = e^{\lambda_r \Delta t} \qquad \lambda_r = \sigma_r + j\, \omega_r \tag{14}$$

$$\sigma_r = \mathrm{Re}\left[\frac{ln\ z_r}{\Delta t} \right] \qquad \omega_r = \mathrm{Im}\left[\frac{ln\ z_r}{\Delta t} \right] \tag{15}$$

Once the matrix coefficients ($[\alpha]$) have been found, the modal frequencies (λ_r or z_r) can be found as the roots of the matrix coefficient polynomial (Equation (11) or (13)) using any one of a number of numerical techniques.

The most commonly used modal identification methods can be summarized as shown in Table 1. The high order model is typically used for those cases where the system is undersampled in the spatial domain. For example, the limiting case is when only one measurement is made on the structure. For this case, the left hand side of the general linear equation corresponds to a scalar polynomial equation with the order equal to or greater than the number of desired modal frequencies. The low order model is used for those cases where the spatial information is complete. In other words, the number of physical coordinates is greater than the number of desired modal frequencies. For this case, the order of the lefthand side of the general linear equation is equal to two. The zero order model corresponds to a cases where the temporal information is neglected and only the spatial information is used. These methods directly estimate the eigenvectors as a first step. In general, these methods are programmed to process data at a single temporal condition or variable. In this case, the method is essentially equivalent to the single-degree-of-freedom (SDOF) methods which have been used with frequency response functions. In others words, the zeroth order matrix polynomial model compared to the higher order matrix polynomial models is similar to the comparison between the SDOF and MDOF methods used historically in modal parameter estimation.

The stabilization or consistency diagram is based upon successive solutions of Equation (11) and Equation (13) for different values of the maximum model order m. In the original historical development, the coefficients of these characteristic polynomial equations were scalar. Since the number of modes is unknown, the model order was increased successively beginning with some minimum number based upon the number of peaks observed in the data. For each increase in model order m, a new set of equations based upon Equation (7) or Equation (10) are formed to solve for a coefficients of the characteristic polynomial. The roots of this characterisitic polynomial are found and these roots (or poles) are identified and compared to the previous set of roots based upon the tolerance values for stability or consistency. Note that if the coefficients are scalar, each increase in model order adds one more root to the number of roots found but the solution is essentially independent from the previous solution. Therefore, all of the roots are found each time, not simply one more root. In current implementations of the consistency diagram, the coefficients are square, either $N_i \times N_i$ or $N_o \times N_o$ so the number of additional roots found by an increase of model order will be either N_i or N_o.

	Domain		Matrix Polynomial Order			Coefficients	
Algorithm	Time	Freq	Zero	Low	High	Scalar	Matrix
Complex Exponential Algorithm (CEA)	•				•	•	
Least Squares Complex Exponential (LSCE)	•				•	•	
Polyreference Time Domain (PTD)	•				•		$N_i \times N_i$
Ibrahim Time Domain (ITD)	•			•			$N_o \times N_o$
Multi-Reference Ibrahim Time Domain (MRITD)	•			•			$N_o \times N_o$
Eigensystem Realization Algorithm (ERA)	•			•			$N_o \times N_o$
Polyreference Frequency Domain (PFD)		•		•			$N_o \times N_o$
Simultaneous Frequency Domain (SFD)		•		•			$N_o \times N_o$
Multi-Reference Frequency Domain (MRFD)		•		•			$N_o \times N_o$
Rational Fraction Polynomial (RFP)		•			•	•	$N_i \times N_i$
Orthogonal Polynomial (OP)		•			•	•	$N_i \times N_i$
Polyreference Least Squares Complex Frequency (PLSCF)		•			•	•	$N_i \times N_i$
Complex Mode Indication Function (CMIF)		•	•				$N_o \times N_i$

TABLE 1. Summary of Modal Parameter Estimation Algorithms

2.2 Common Consistency Diagram Concepts

As described before, the consistency diagram is developed by successively computing different model solutions (utilizing different model order for the characteristic polynomial, different normalization methods for the characteristic matrix coefficient polynomial, different equation condensation methods and/or different algorithms) and involves tracking the estimates of frequency, damping, and possibly modal vectors (modal participation vectors) as a function of model solution iteration. If only model order is evaluated, recent research [6-10] has shown that the correct choice of normalization of the matrix coefficient, characteristic polynomial has a distinct affect on producing clear consistency diagrams. This research noted that the characteristic polynomial should be normalized so that the lowest order coefficient is unity (scalar coefficient polynomial) or the lowest order coefficient matrix is the identity matrix (matrix coefficient polynomial) [8]. This will be referred to as low order normalization subsequently in the rest of this paper.

Historical methods commonly normalized the highest order coefficient (high order normalization) or, in some cases, alternatively used both (low and high order normalization). When low order normalization is used, many of the spurious poles that are found, due to the noise on the data, are located in the right half S-plane where the damping is not realistic. These poles are generally excluded since they are not physically possible in a passive structural system. Nevertheless, the nonphysical (computational) poles will not be estimated in a consistent way during this process and can be sorted out of the modal parameter data set more easily. Note that inconsistencies (frequency shifts, leakage errors, etc.) in the measured data set will obscure this consistency and render the diagram difficult to use.

Figures 3 through 5 demonstrate three different presentations of consistency diagrams based upon different normalizations of the characteristic matrix coefficient polynomial. In all three figures, an average autopower of the FRF(s) is plotted on the consistency diagram in the background for reference.

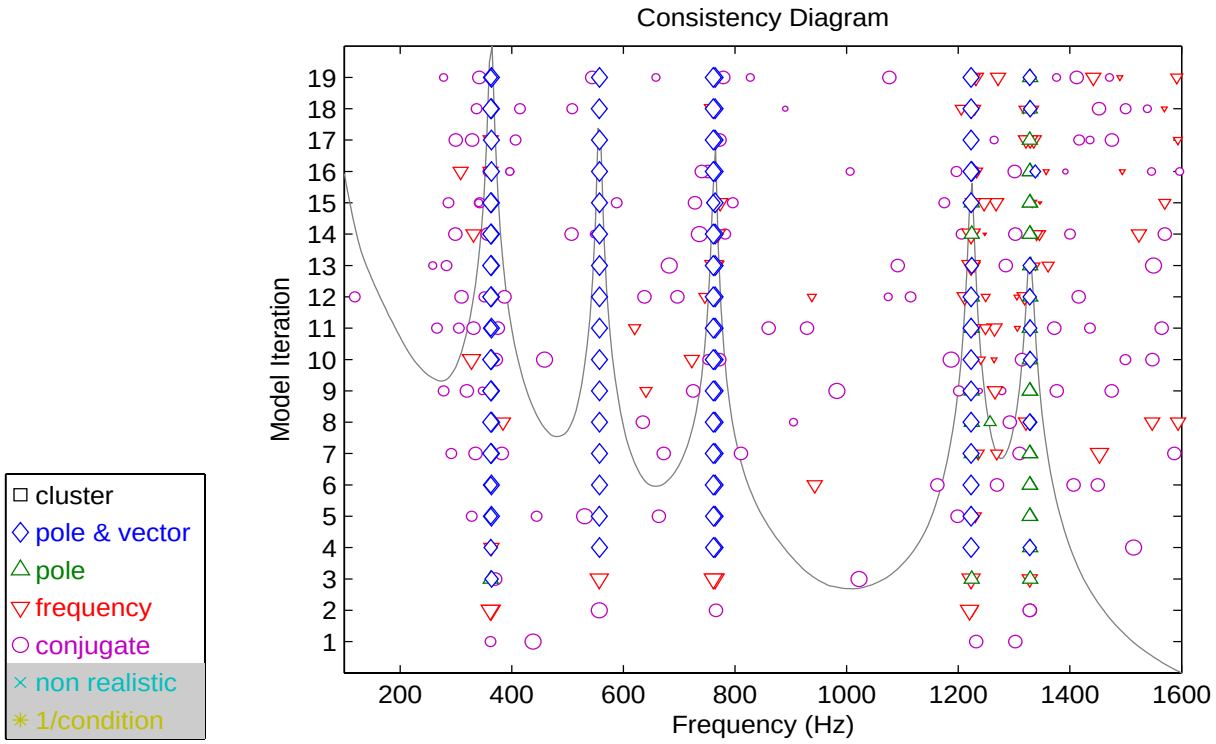

Figure 3. Consistency Diagram (RFP) - High Order Coefficient Normalization

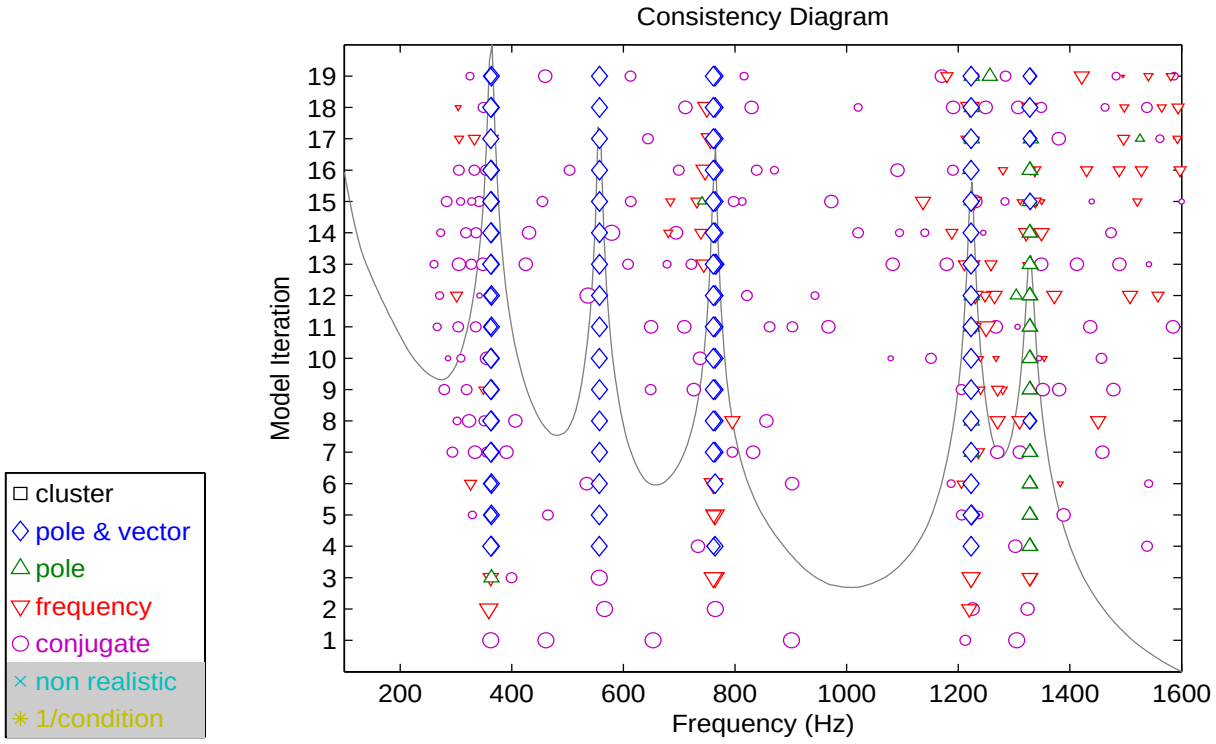

Figure 4. Consistency Diagram (RFP) - Low Order Coefficient Normalization

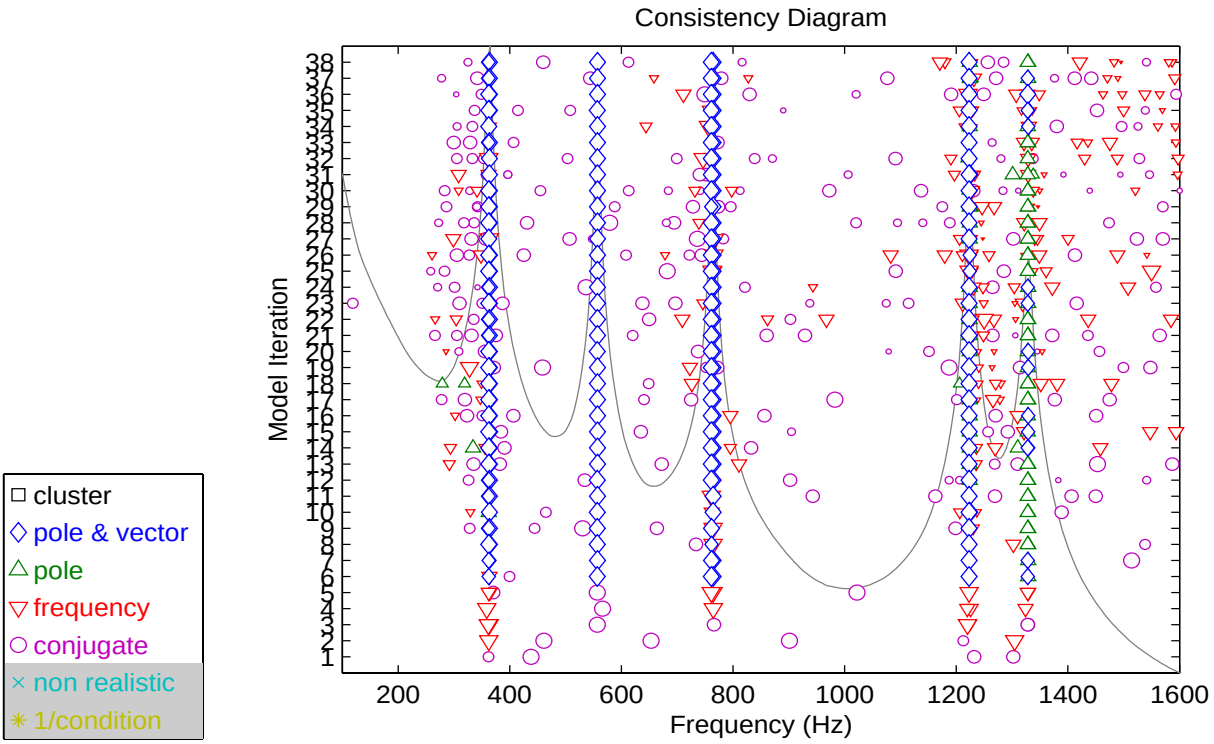

Figure 5. Consistency Diagram (RFP) - Both Normalizations

A number of recent papers [5,7,8,12,13] have identified the effects of changing the consistency tolerances on the resultant consistency diagrams, yielding a clearer presentation of symbols that indicate the presence of a structural mode of vibration. This process of altering the look of the consistency diagram by altering the consistency tolerances will not be reviewed further here. Note that there are other pole presentation diagrams, related to the consistency diagram, such as Pole Surface Consistency and Pole Surface Density diagrams that have proven useful for identifying modal parameters [11-13] and may be more powerful than the consistency diagram alone. Since the poles that are compared on these pole surface diagrams are generally limited to the poles identified on the consistency diagram, they will not be reviewed here either. An example of these Pole Surface Diagrams are given in Figures 6-9.

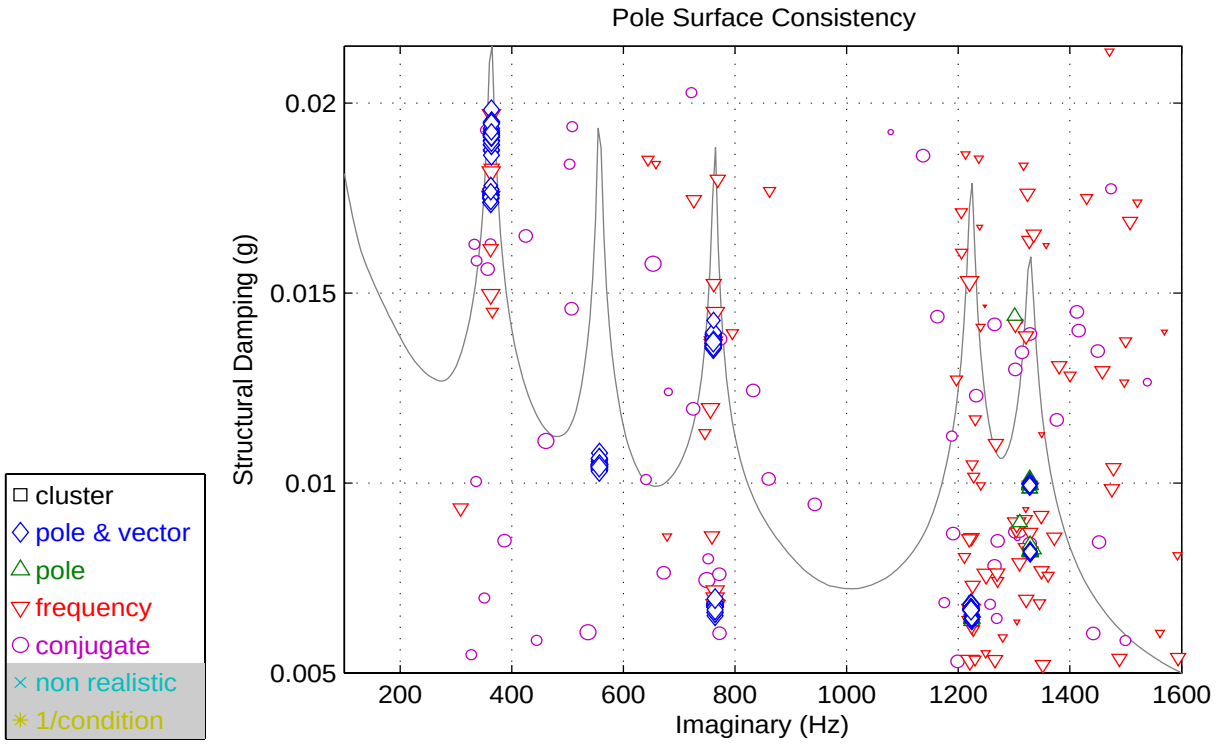

Figure 6. Pole Surface Consistency Diagram (RFP) - Both Normalizations

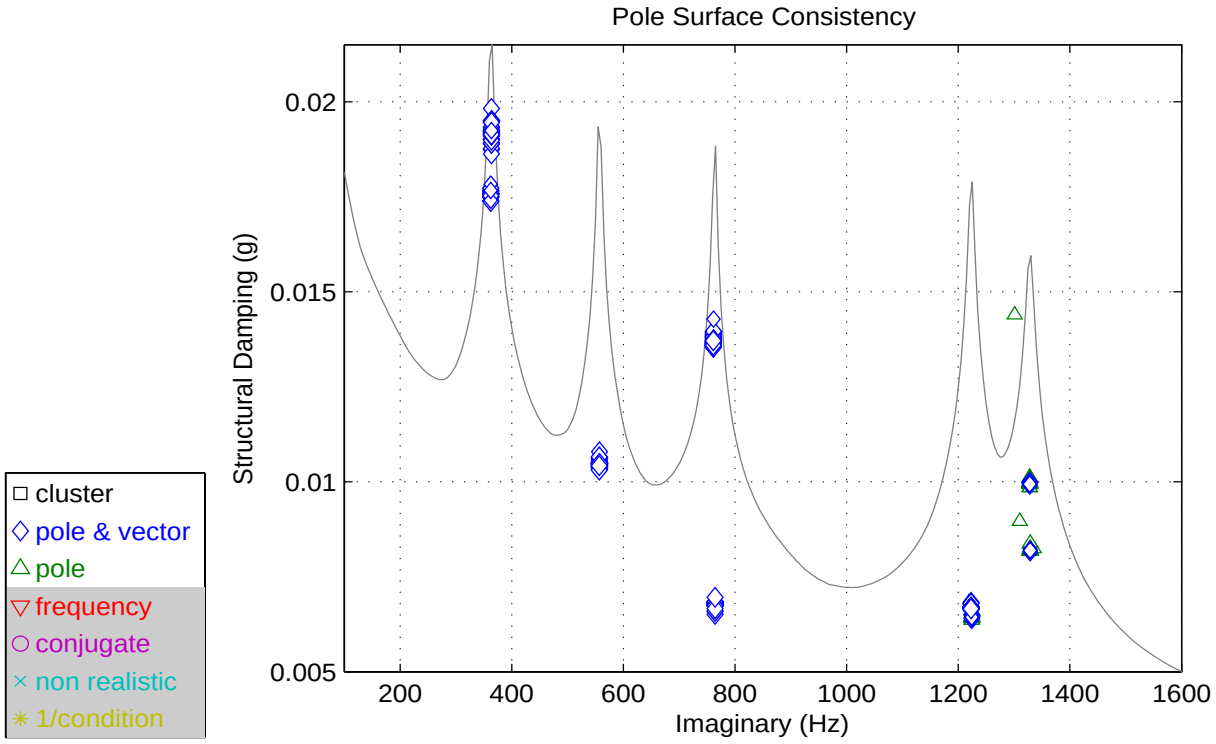

Figure 7. Pole Surface Consistency Diagram (RFP) - Both Normalizations - Conjugate & Frequency Suppressed

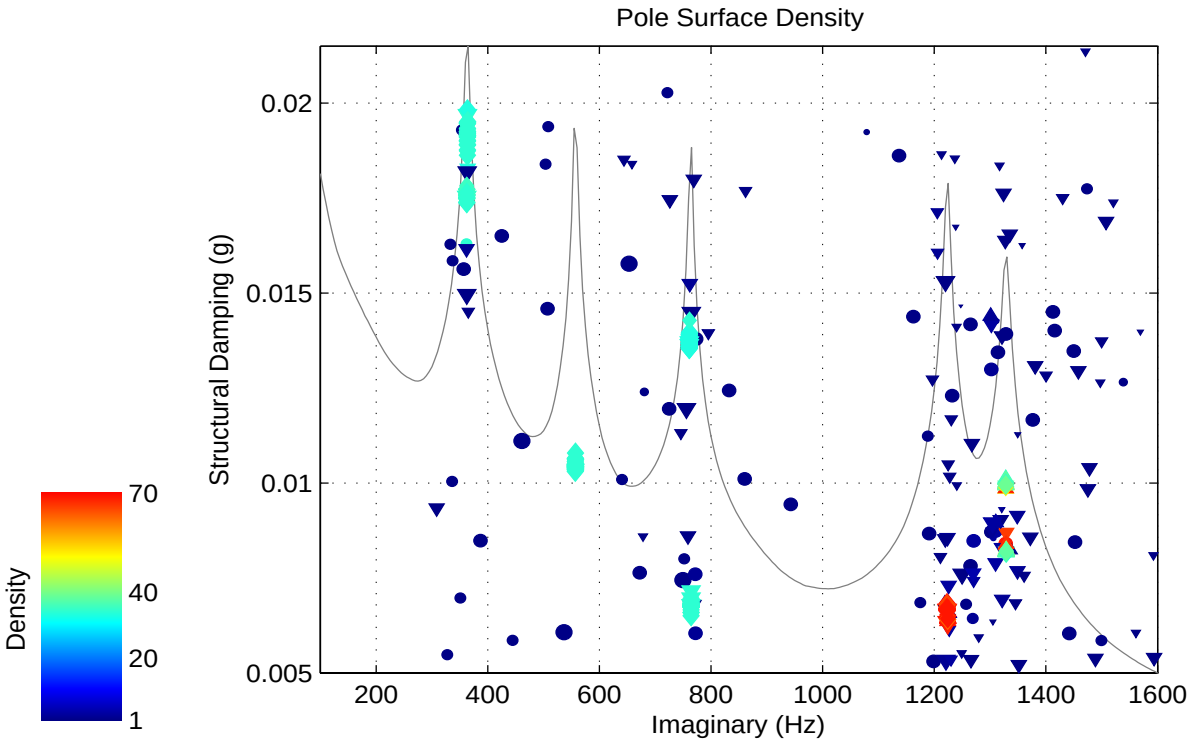

Figure 8. Pole Surface Density Diagram (RFP) - Both Normalizations

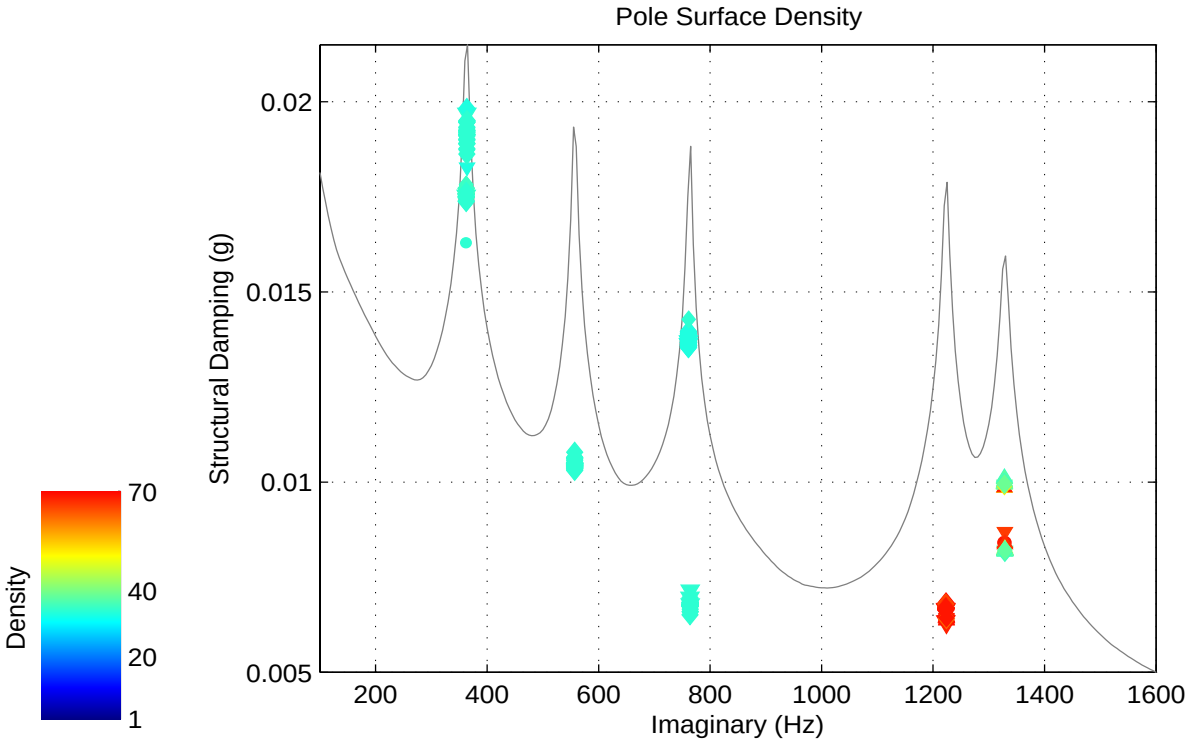

Figure 9. Pole Surface Density Diagram (RFP) - Both Normalizations - Isolated Single Poles Suppressed

Figure 10 is the same as data as Figure 5 with the symbols indicating conjugate poles and frequency consistency suppressed. Note that in all cases, suppressing the obvious spurious computational poles

results in a substantially cleaner consistency diagram with clear indications of the pole locations.

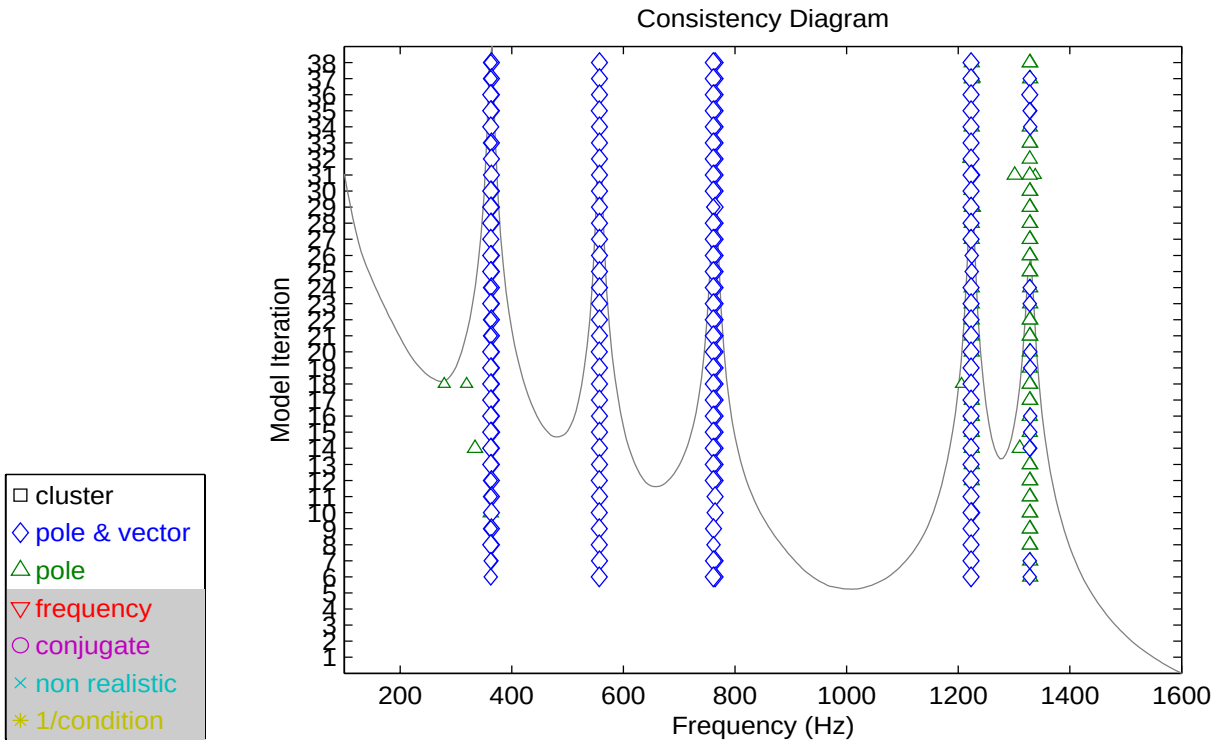

Figure 10. Consistency Diagram (RFP) - Both Normalizations - Conjugate & Frequency Suppressed

Note that in the previous figure, the consistency diagram, in the ordinate direction, changed both the normalization method and the model order in successive fashion. This generalization of the stability or consistency diagram is very important. In the following section of this paper, the vertical axis will be used to indicate successive increase in the denominator polynomial (characteristic polynomial associated with complex-valued modal frequencies), to indicate successive increase in the order of the numerator polynomial (residues and residuals), to indicate different normalization methods (frequency and coefficient) and to indicate a sequence of combinations of all of these iterations. This will be identifed in each following example.

3. Additional Clear Consistency Diagram Methods

A number of different methods can be used to generate the consistency diagram that will impact the clarity of the consistency diagram. These methods can be combined with the coefficient normalization and consistency tolerances to generate a very clear diagram in most cases where the measured data has a reasonable match to linear, reciprocal system assumptions, observability issues and reasonable data noise levels. The methods described in the following sections have been used on a wide range of data cases in the automotive and aerospace application areas with good success. The methods that will be discussed are:

- Symbol Sizing Based Upon Normal Mode Criteria
- Complete or Incomplete Vector Comparisons
- Using Both Coefficient Normalization Methods

- Numerator and Denominator Model Order Variation [14]
- Fixed Denominator and Numerator Order Variation [14]
- Frequency Normalization Variation

The details of these methods will be further discussed in the following sections using the same data cases. The data case chosen for this comparison is based upon measurements made on a simple circular plate. In the frequency range of analysis, there will be either five or nine modes present and all but one mode will be in repeated root pairs. This data is very simple and the answers for the modal parameters correspond well to analytical models of the system and previous testing done on the structure. There is little measurement noise on the measured FRF data and the data are nearly ideal. However, many more poles will be estimated (compared to the number of known modes) as model order is increased and the clarity of using different presentation methods will be apparent, even with this simple case.

Since many modal parameter estimation algorithms are developed on the basis of either the number of inputs (N_i) or the number of outputs (N_o), assuming that one or the other is larger based upon test method, some nomenclature conventions are required for ease of further discussion. In terms of the modal parameter estimation algorithms and the ultimate matrix coefficient, characteristic polynomial equation, it is more important to recognize whether the algorithm develops the square matrix coefficient on the basis of the larger of N_i or N_o or the smaller of N_i or N_o. For this reason, the terminology of long (larger of N_i or N_o) dimension or short (smaller of N_i or N_o) dimension is easier to understand without confusion. Using this approach, PTD, RFP and PLSCF are all short dimension methods where the vector found as part of the solution for poles is very small while ERA and PFD are long dimension methods where the vector found as part of the solution for poles is of full length, based upon measurement locations.

3.1 Symbol Size and Long Vector Effects

In this first set of examples, the symbol size for each consistency evaluation is altered based upon a comparison of the Mean Phase Coefficient (MPC) computed on the basis of the vector found with each pole. The Mean Phase Coefficient is a normailized measure of how close the normalized vector is to a real-valued vector. Since normal modes are often expected in modal parameter estimation, this can be used as an effective way to screen possible solutions that do not meet this case. The Mean Phase Coefficient (MPC) is a number between 0 and 1 where 1 indicates a completely normal (real-valued) vector. The Mean Phase Coefficient (MPC) is computed as follows:

$$MPC = 1 - \frac{||Imag\ (\{\psi\}\ e^{-j\phi})||}{||Real\ (\{\psi\}\ e^{-j\phi})||} \tag{16}$$

where ϕ is defined as the weighted mean vector angle.

Depending upon the modal parameter estimation algorithm used, this vector may be of long or short dimension. When using PTD, RFP or PLSCF methods, this short dimension may only be 2 or 3 yielding the computation of MPC very sensitive and statistically insignificant.

A comparison of the relative consistency information for a PTD algorithm, presented through changes in symbol size based upon MPC and the calculation of long basis residue vectors, is presented in Figures 11-14. Figure 11 shows the basic normal PTD consistency. Figure 12 shows the same basic normal PTD consistency, however the MAC calculation is based upon long basis residue vectors. For this case, comparison of a short basis participation vector MAC with a long basis residue vector MAC, no obvious significant additional consistency information is presented. (Note that although the consistency diagram itself doesn't indicate more information, an animation of the two vectors would provide greater visual assistance for the long basis vectors.)

Figure 13 presents the same results as Figure 11, however now the symbols are scaled by the MPC. The

addition of symbol size helps to differentiate those solutions that most closely match a normal mode. Figure 14 presents the same results as Figure 12, however again the symbols are scaled by the MPC. Overall, the comparison of Figures 11-14 indicate that while the standard consistency indicators do not change for each calculated pole, the symbol size provides an indication of those poles which, while stable according to traditional criteria, may be more poorly estimated. Comparing the symbol size information for the modes between 300 and 800 Hz with the symbol size for the modes between 1200 and 1400 Hz, reveals that the lower band symbols are all clearly larger than those of the upper band indicating that the modes estimated in the lower band are all more nearly normal (i.e. less complexity) and may perhaps be better estimated.

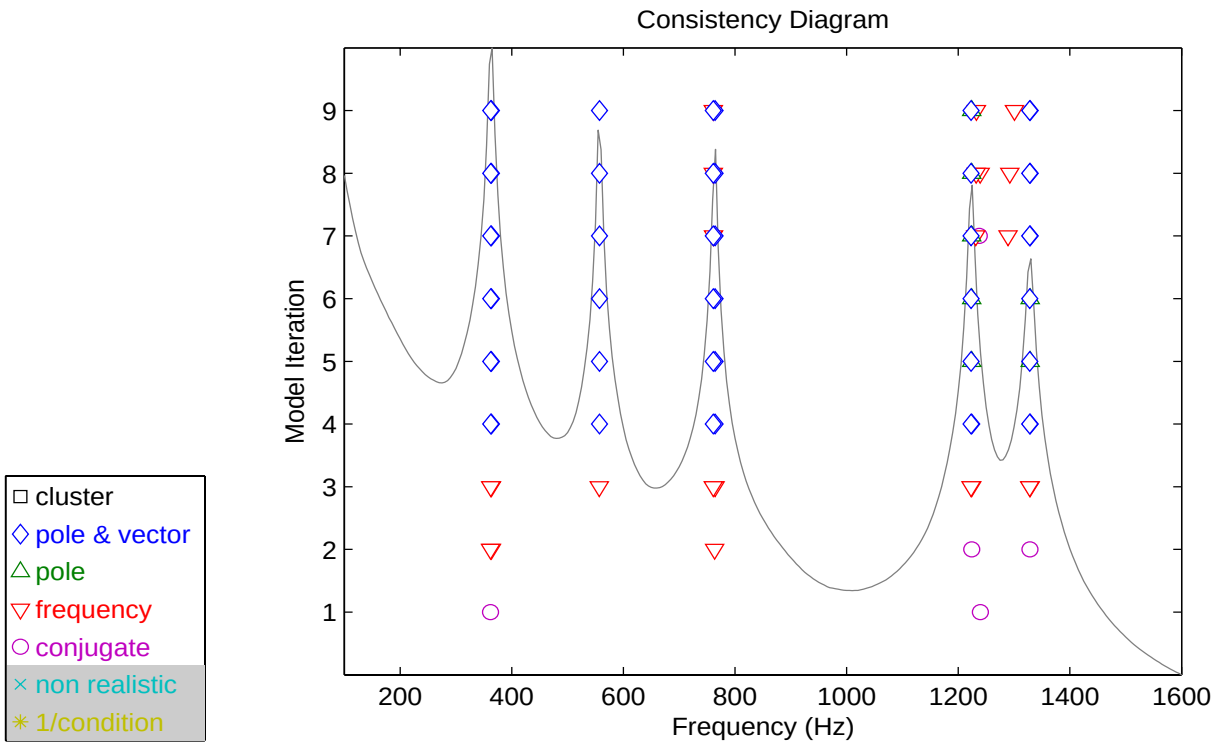

Figure 11. PTD, Short Basis, No Symbol Resize

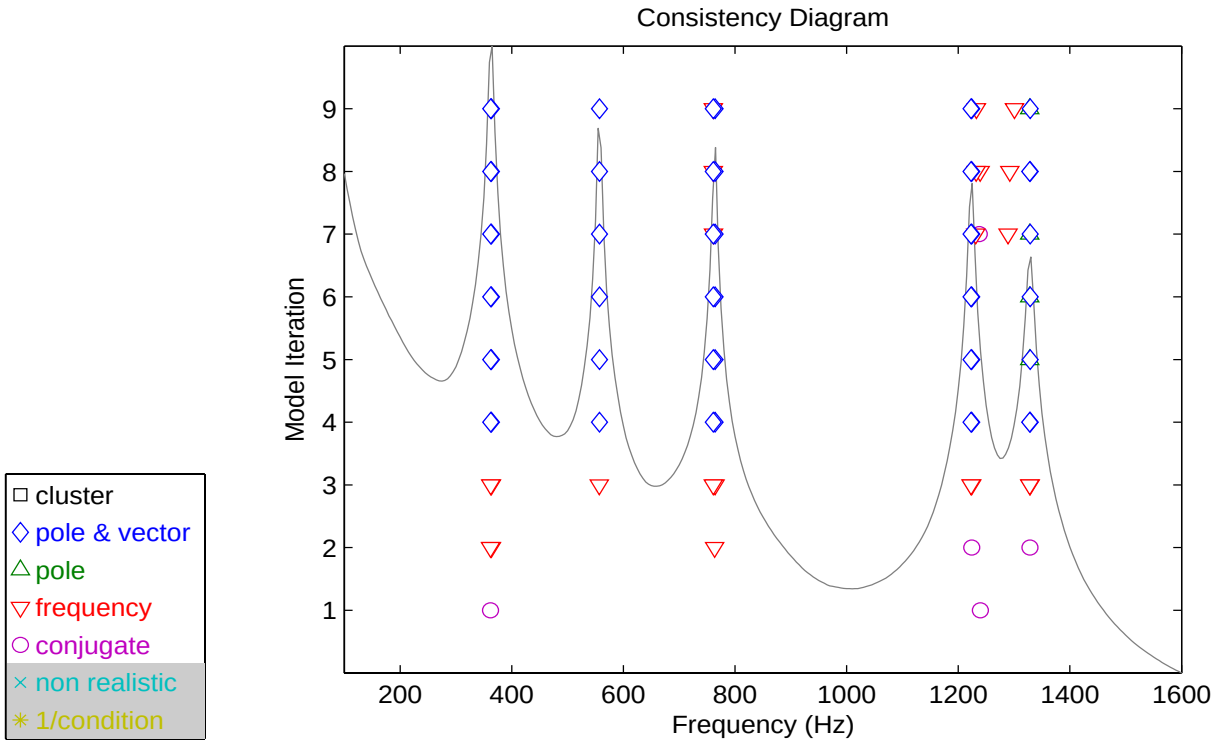

Figure 12. PTD, Long Basis, No Symbol Resize

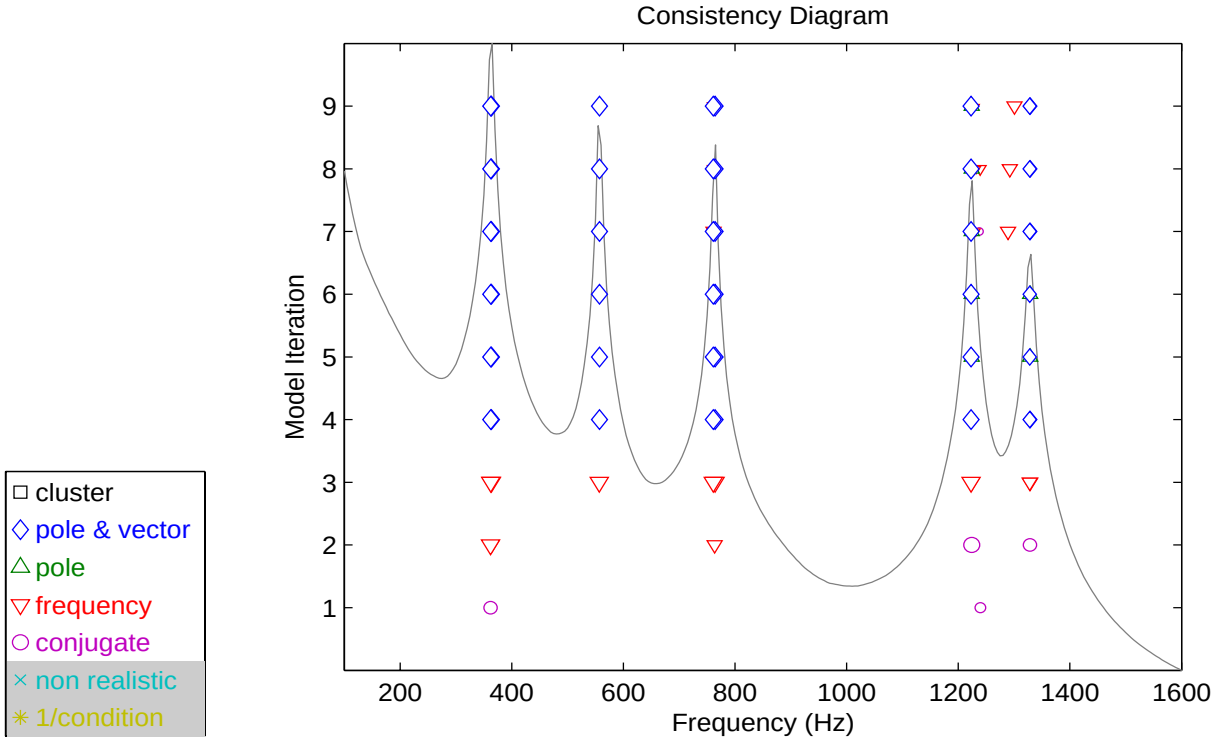

Figure 13. PTD, Short Basis, Symbol Resize on Mean Phase Coefficient

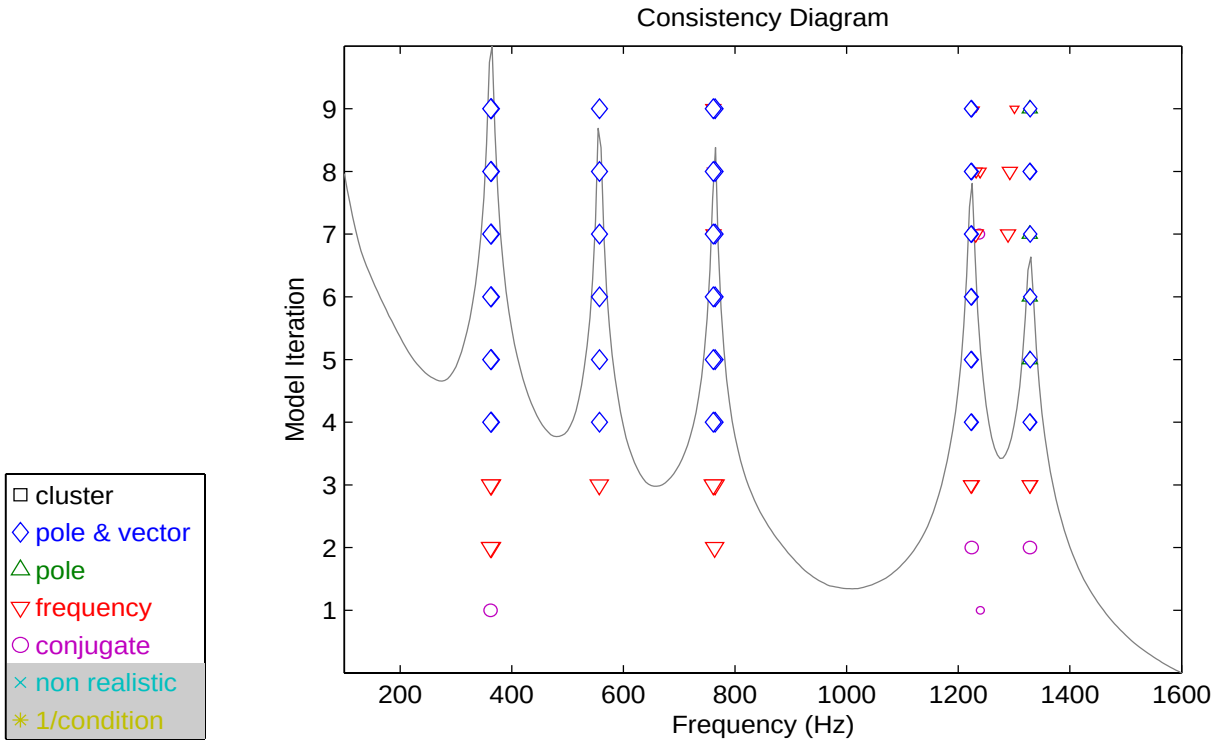

Figure 14. PTD, Long Basis, Symbol Resize on Mean Phase Coefficient

3.2 Coefficient Normalization - Both

In this second set of examples, the effect of coefficient normalization is presented. For the four cases shown, the first, Figure 15, shows the consistency as traditionally presented using high order coefficient normalization. The second case, Figure 16, shows the consistency as currently advocated using low order coefficient normalization. Third, Figure 17, the two coefficient normalization approaches are interleaved where for successive model iterations, first the normalization is varied and second the model order is increased. The fourth, Figure 18, shows the visual improvement obtained by simply suppressing the isolated conjugate poles.

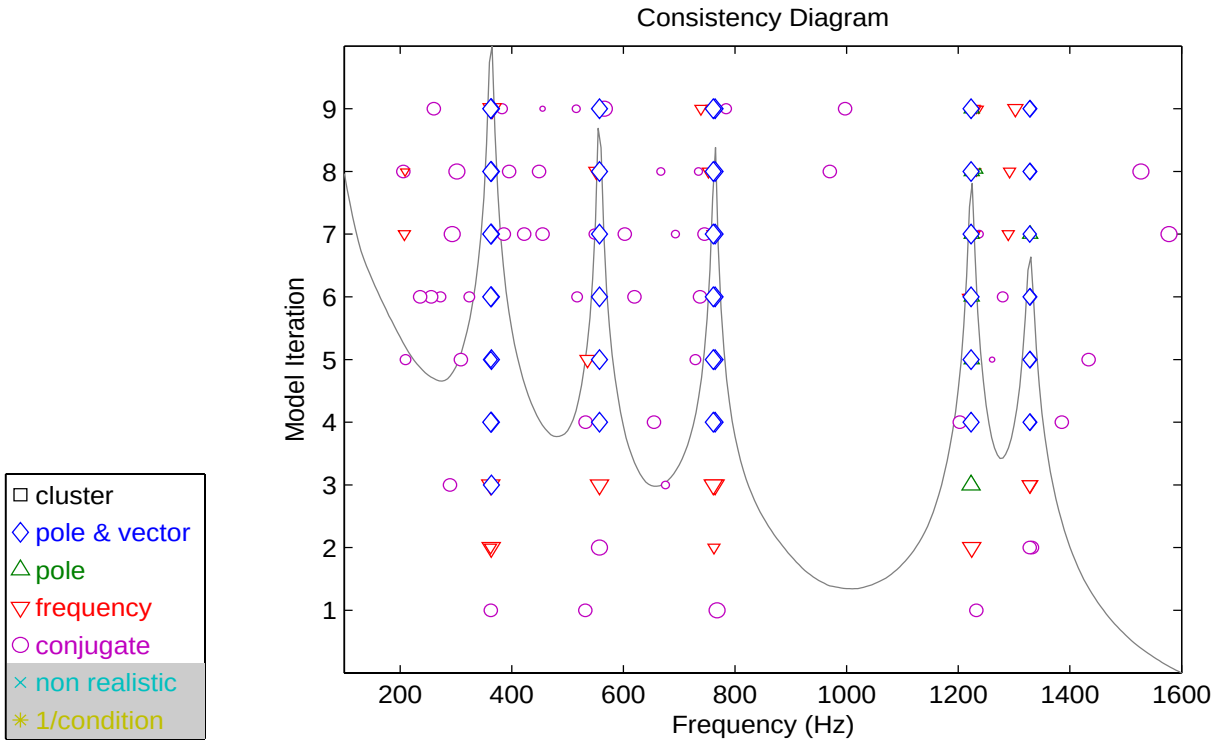

Figure 15. PTD, Short Basis, High Order Coefficient Normalization

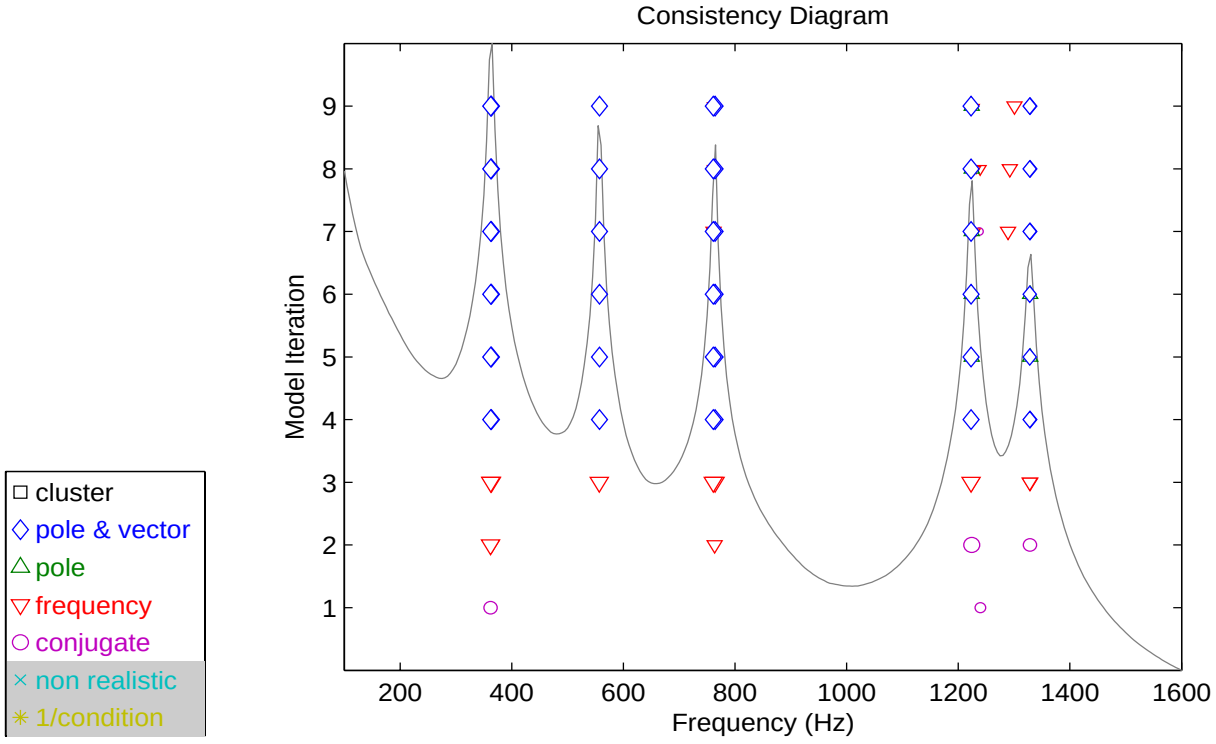

Figure 16. PTD, Short Basis, Low Order Coefficient Normalization

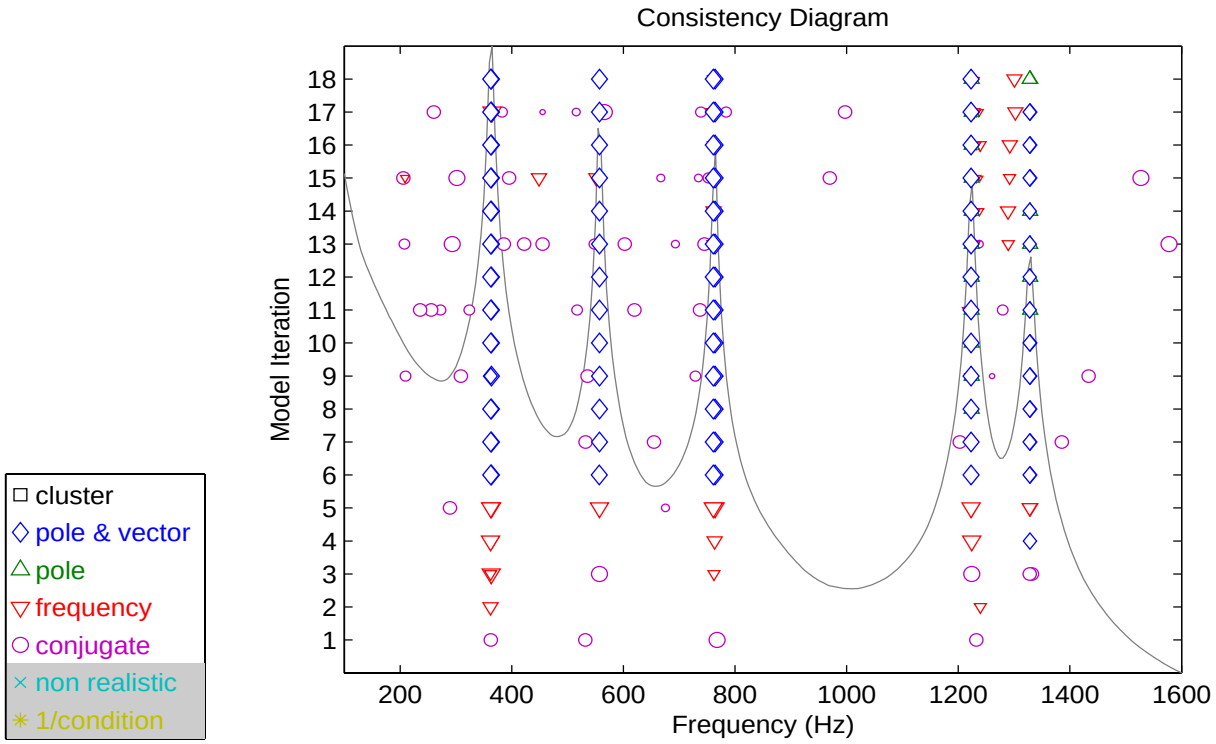

Figure 17. PTD, Short Basis, Alternating High/Low Order Coefficient Normalization

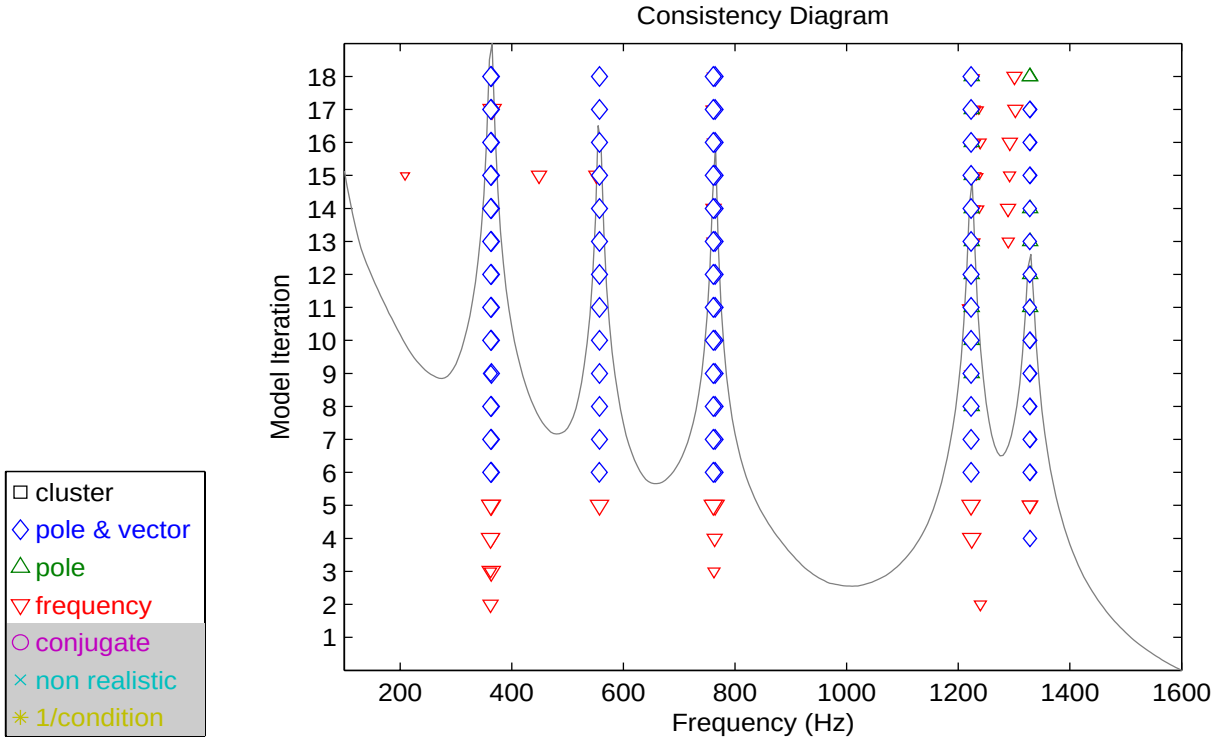

Figure 18. PTD, Short Basis, Alternating High/Low Order Coefficient Normalization, No Conjugate Symbol

It should be noted here that the equation formulation used in this presentation assumes that the negative frequency portion of the FRF is the complex conjugate of the positive frequency data. This forces the solution to always yield roots in complex conjugate pairs. Hence, both the roots due to structural modes and the roots due to noise will also always occur in complex conjugate pairs. Therefore, it is reasonable to suppress any symbol associated with a solution which occurs as an isolated conjugate pole pair.

3.3 Numerator Polynomial Evaluation

Frequently, the number of modes present in the data in a given frequency range can be estimated with reasonable accuracy. This can occur when there is significant *a priori* knowledge of the structure via previous testing and/or modeling or knowledge based upon a mode indicator function. When this occurs, the model order of the denominator, essentially the characteristic polynomial, can be chosen or limited to a very small range of choices. In this situation, rather than incrementing the model order of the denominator polynomial on the vertical axis of the consistency diagram, it is more useful to increment the model order of the numerator polynomial. This effectively alters the number of residuals used to account for the out-of-band modes and noise rather than increasing the number of poles which have to be sorted. This approach has been shown to work well in cases with significant measurement noise, like civil structures, and has been documented previously [14] . Unfortunately, though, this approach is not used in many commercial implementations.

Overdetermining the denominator model order versus overdetermining the numerator model essentially involves the convolution of the numerator and denominator polynomial terms as described in the following development. Starting with the basic polynomial model for $H(s)$:

$$[H(s)] = \left[\sum_{k=0}^{m}\left[\alpha_k\right](s)^k\right]^{-1}\left[\sum_{k=0}^{n}\left[\beta_k\right](s)^k\right] \tag{17}$$

Adding a generalized residual polynomial results in:

$$[H(s)] = \left[\sum_{k=0}^{n}\left[\alpha_k\right](s)^k\right]^{-1}\left[\sum_{k=0}^{m}\left[\beta_k\right](s)^k\right] + \left[\sum_{k=n_l}^{n_u}\left[R_k\right](s)^k\right] \tag{18}$$

The residual polynomial can be combined with the numerator polynomial (β) by convolving the residual polynomial (R) with the demonator polynomial (α) and adding equivalent terms.

First multiplying by the (α) polynomial:

$$[H(s)] = \left[\sum_{k=0}^{n}\left[\alpha_k\right](s)^k\right]^{-1}\left(\left[\sum_{k=0}^{m}\left[\beta_k\right](s)^k\right] + \left[\sum_{k=0}^{n}\left[\alpha_k\right](s)^k\right]\left[\sum_{k=n_l}^{n_u}\left[R_k\right](s)^k\right]\right) \tag{19}$$

Re-writing the convolved α-R polynomial as $\hat{R}$:

$$[H(s)] = \left[\sum_{k=0}^{n}\left[\alpha_k\right](s)^k\right]^{-1}\left(\left[\sum_{k=0}^{m}\left[\beta_k\right](s)^k\right] + \left[\sum_{k=n_l}^{n+n_u}\left[\hat{R}_k\right](s)^k\right]\right) \tag{20}$$

Then combining $\hat{R}$ polynomial with the β polynomial and expressing as $\hat{\beta}$ yields:

$$[H(s)] = \left[\sum_{k=0}^{n}\left[\alpha_k\right](s)^k\right]^{-1}\left[\sum_{k=\min(0,n_l)}^{max(m,n+n_u)}\left[\hat{\beta}_k\right](s)^k\right] \tag{21}$$

Assuming that $n_l \leq 0$, $n_u \geq 0$, and $m \leq n$, then the expression simplifies to:

$$[H(s)] = \left[\sum_{k=0}^{n}\left[\alpha_k\right](s)^k\right]^{-1}\left[\sum_{k=n_l}^{n+n_u}\left[\hat{\beta}_k\right](s)^k\right] \tag{22}$$

In this example, Figures 19-25, the effect of the addition of residuals to the normalized frequency (RFP) and Z transformed frequency (RFPZ) solutions is presented. The RFPZ solution is based upon the PLSCF or PolyMAX ® development.

For this example, there are five poles in band and the data used has seven references. Therefore, ideally, the model order required to reliably identify the poles should be two. However, as will be obvious in the plot sequence, the ability to identify the poles at minimum model order is dependent upon the residual polynomial used to account for out-of-band contributions. For comparison purposes, a PTD algorithm solution, Figure 19, is presented to show that a denominator polynomial order of two is sufficient for solution.

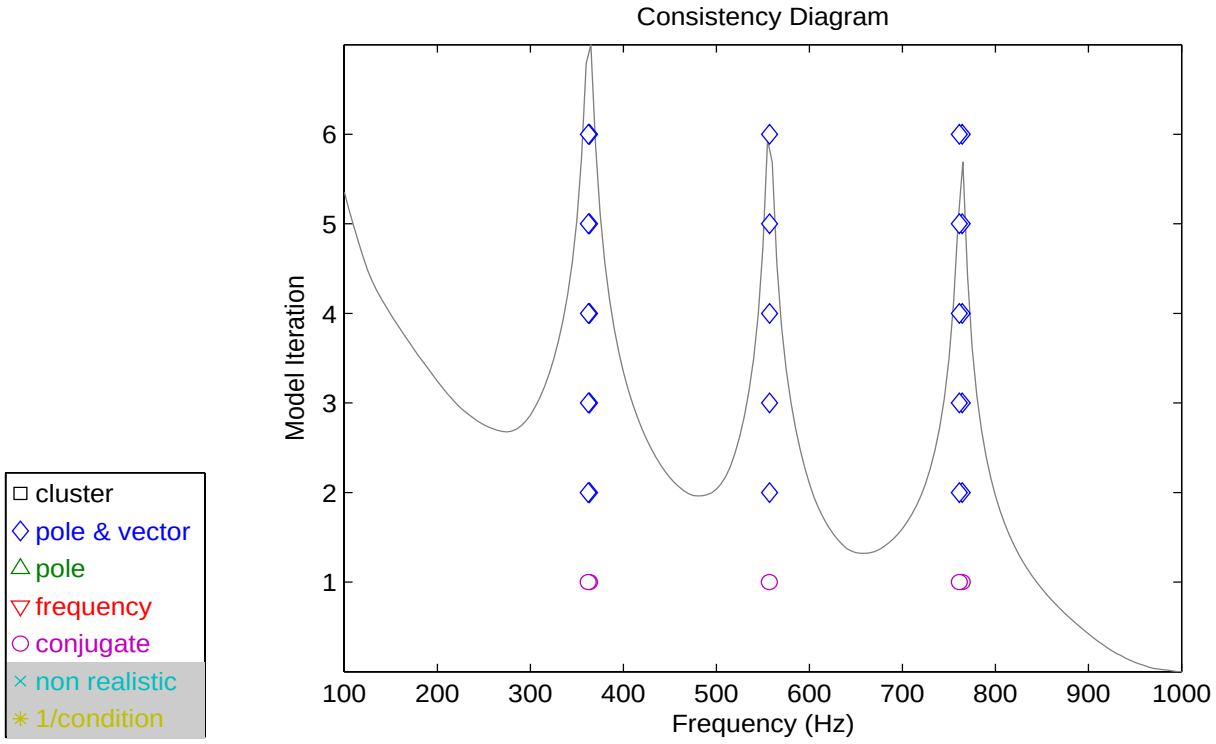

Figure 19. PTD, Short Basis, Low Order Coefficient Normalization

For the RFP algorithm, Figures 20-22, the plot sequence demonstrates the importance and influence of the residual polynomial on the computed poles. While it is possible to get consistent pole estimates by increasing model order, having the correct residual polynomial provides a clear consistency indication at the expected model order. As was to be expected for a frequency domain solution, the ideal residual polynomial model included traditional residual flexibility and inertance terms.

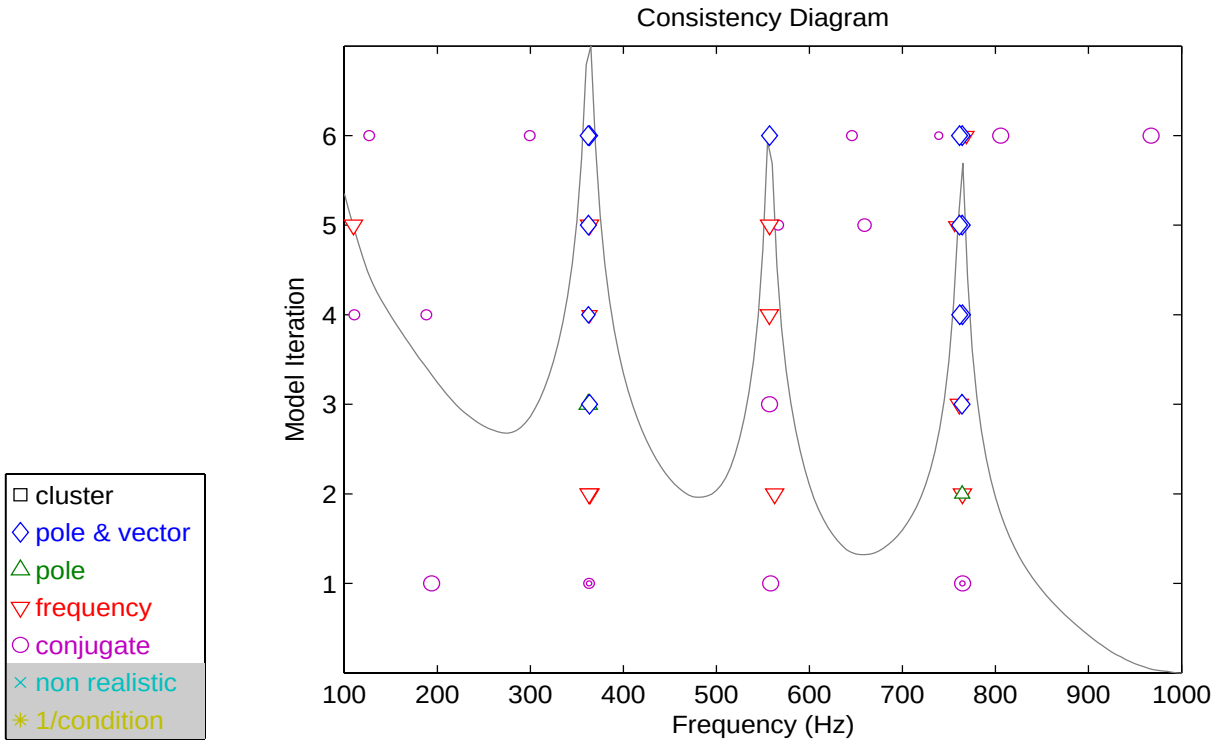

Figure 20. RFP, Short Basis, Low Order Coefficient Normalization, No Residuals

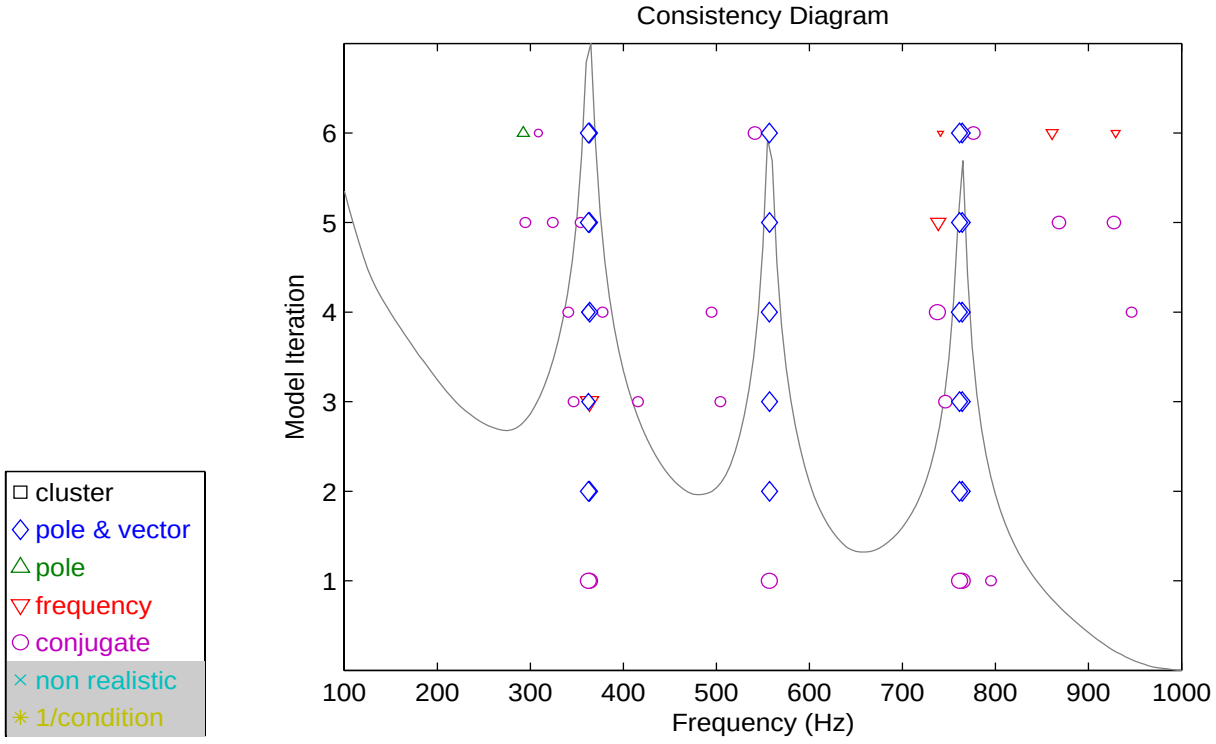

Figure 21. RFP, Short Basis, Low Order Coefficient Normalization, (0,-2) Residuals

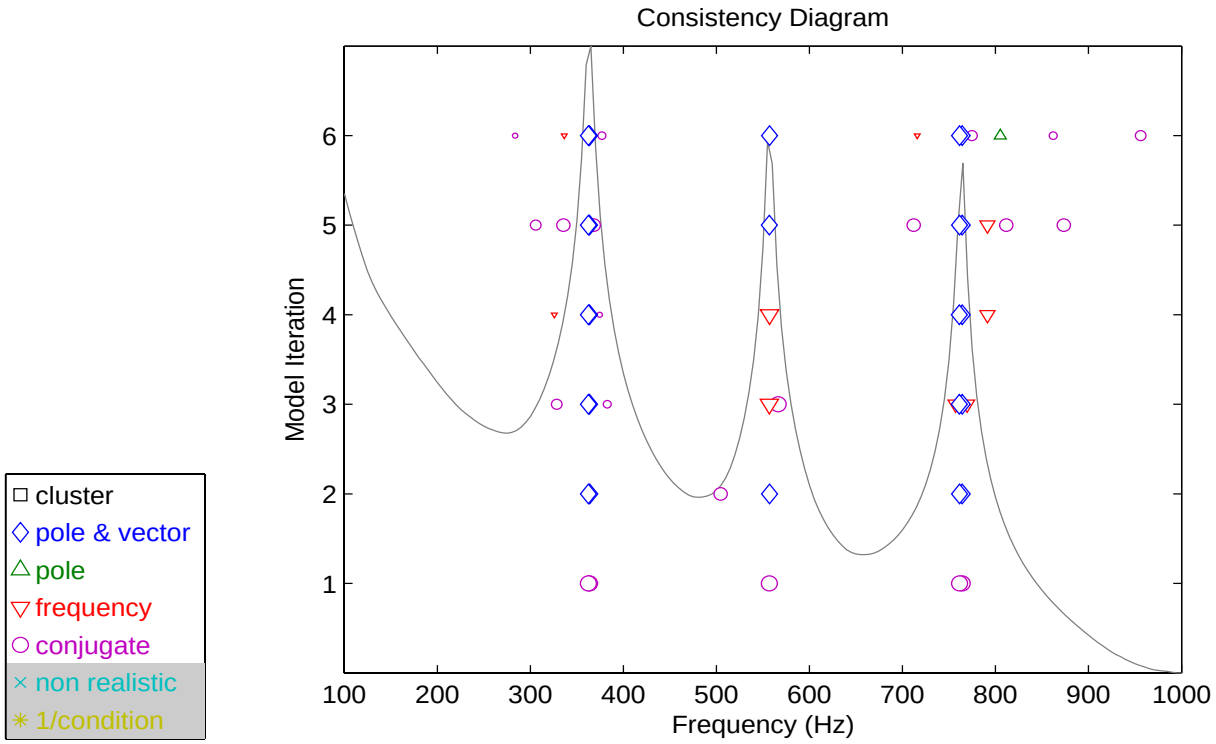

Figure 22. RFP, Short Basis, Low Order Coefficient Normalization, (2,-4) Residuals

For the RFPZ algorithm, Figures 23-25, just as with the RFP algorithm, the plot sequence demonstrates the importance and influence of the residual polynomial on the computed poles. Again, while it is possible to get consistent pole estimates through increasing model order, having the correct residual polynomial provides a clear consistency indication at the expected model order. However, unlike the normalized frequency domain RFP algorithm, the plots reveal that for the Z transformed frequency solution, the ideal residual polynomial model requires more than simply residual flexibility and inertance; in this case higher order residual polynomial terms are required as well.

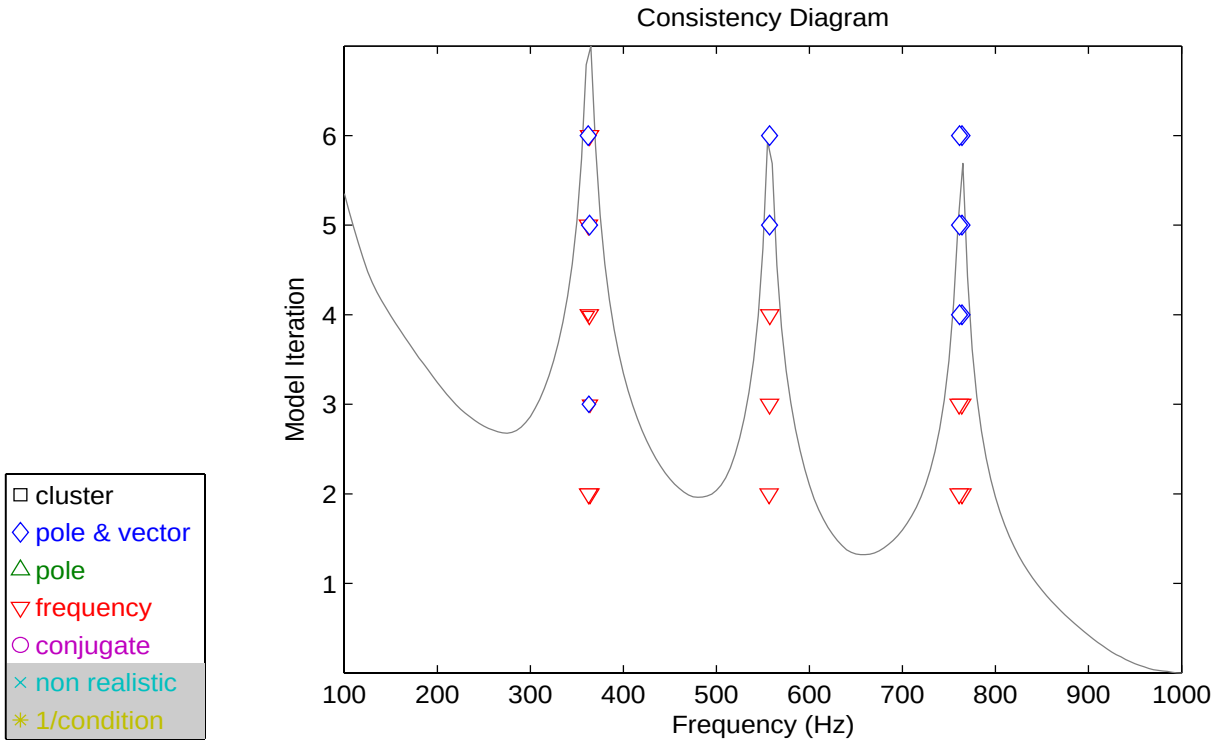

Figure 23. RFPZ, Short Basis, Low Order Coefficient Normalization, No Residuals

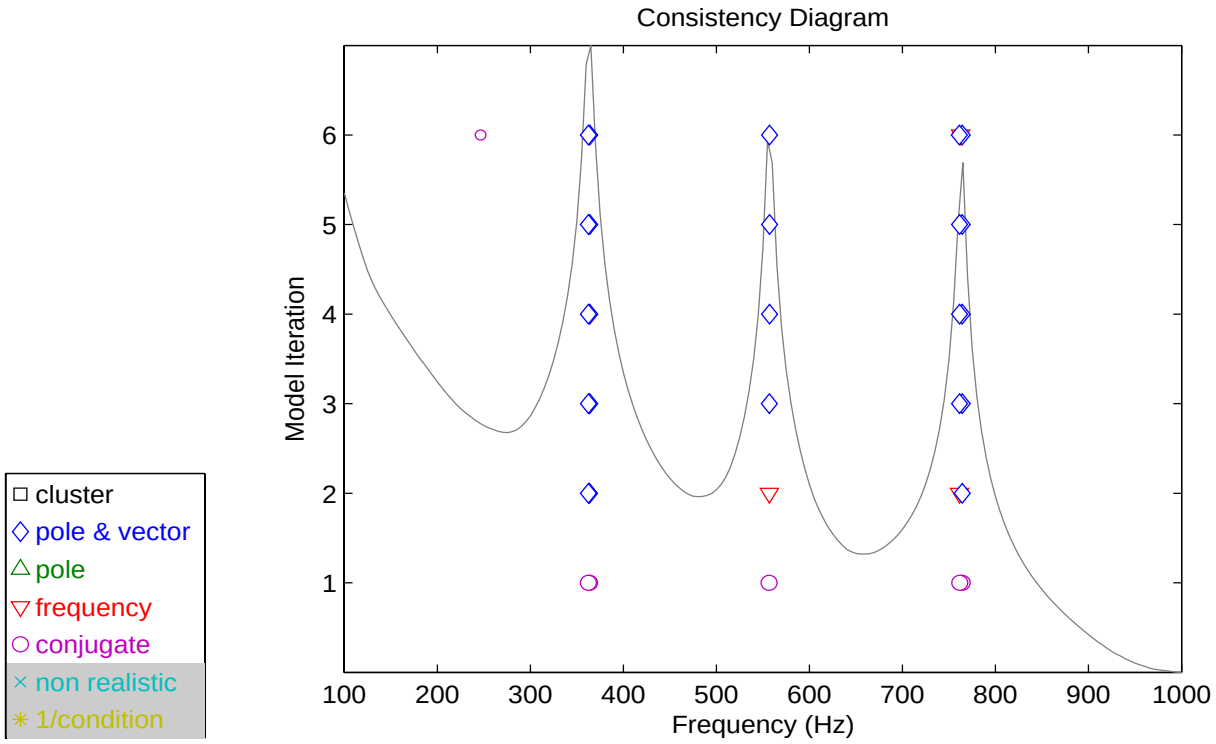

Figure 24. RFPZ, Short Basis, Low Order Coefficient Normalization, (0,-2) Residuals

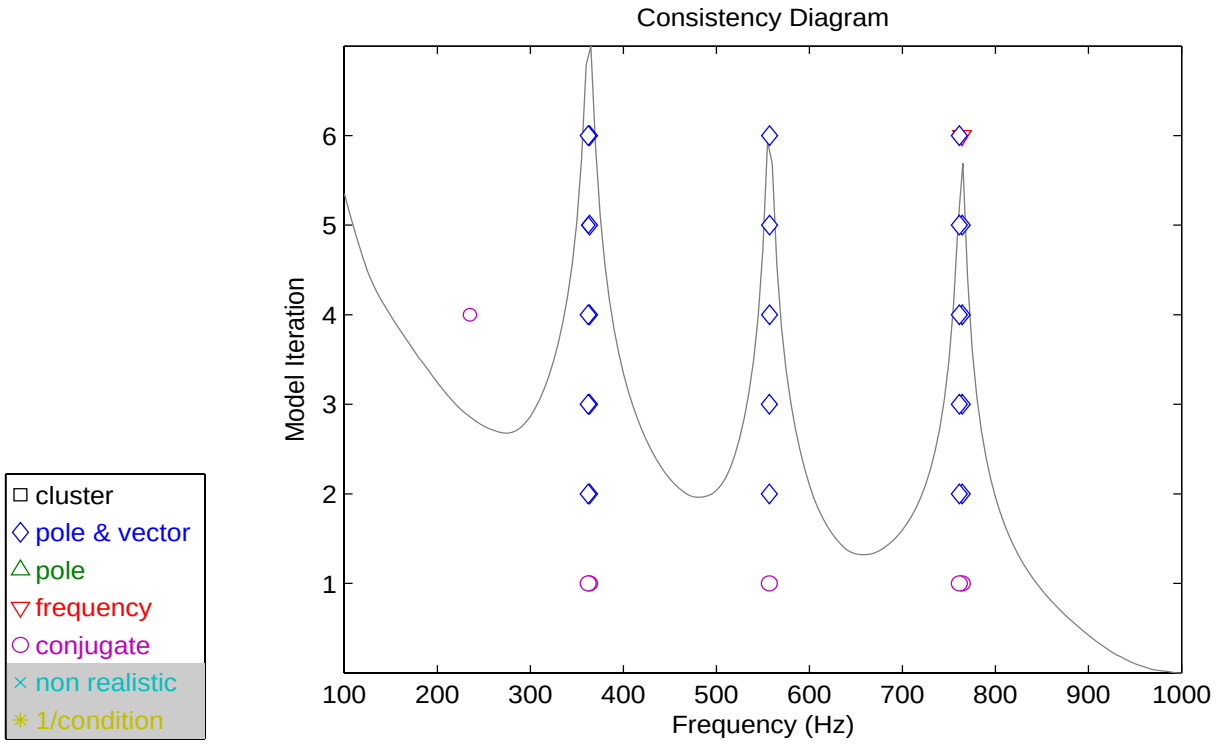

Figure 25. RFPZ, Short Basis, Low Order Coefficient Normalization, (2,-4) Residuals

3.4 Fixed Denominator, Successive Numerator Model Order

In contrast with the previous example where the residual model order was fixed and model iteration was still over varying denominator model order, in this example, Figures 26 and 27, recognition of the fact that ideally a denominator model order of two should be sufficient is used. For this example, the denominator model order is fixed at two and it is the residual polnomial model order which is varied. As is appearent in the figures, once the correct residual order is achieved, the five poles are calculated reliably. This technique has been used effectively on a number of civil engineering structures where there was clear indication of the number of poles present, but there was also significant noise as well.

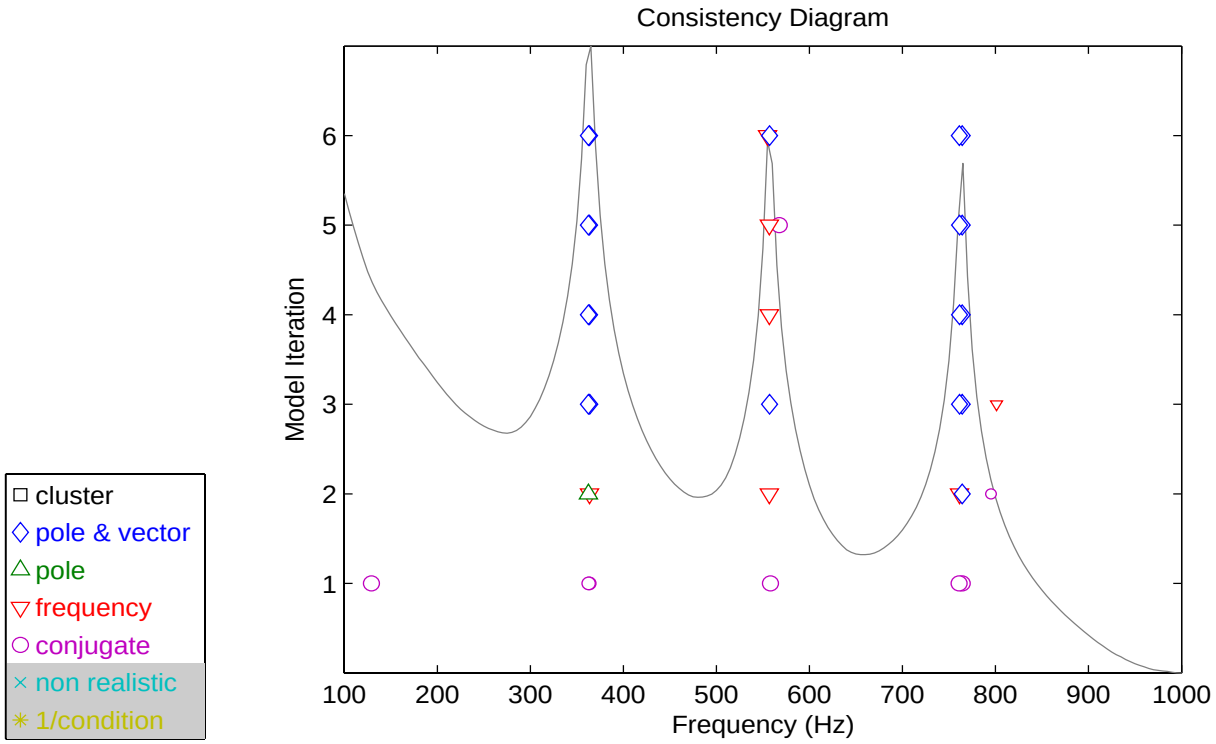

Figure 26. RFP, Short Basis, Low Order Coefficient Normalization, Model Order 2 Denominator, (0,0), (0,-2), (1,-3), (2,-4), (3,-5), (4,-6) Residuals

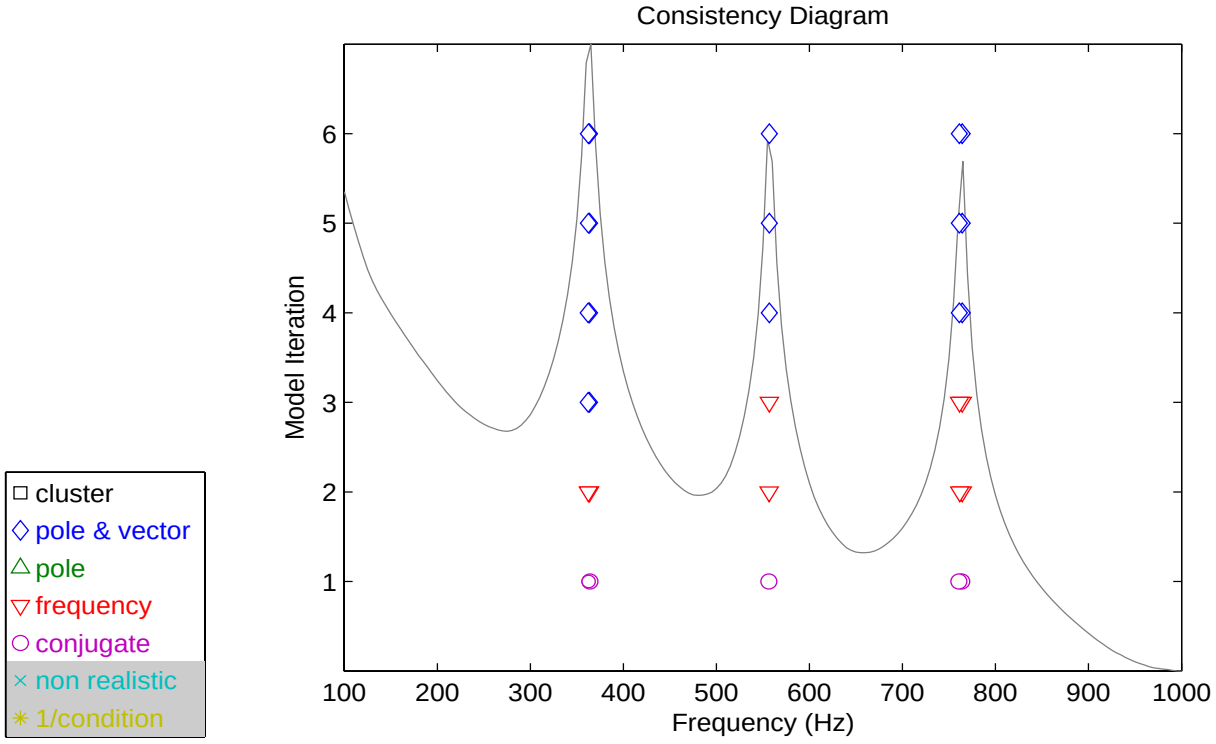

Figure 27. RFPZ, Short Basis, Low Order Coefficient Normalization, Model Order 2 Denominator, (0,0), (0,-2), (1,-3), (2,-4), (3,-5), (4,-6) Residuals

3.5 Frequency Normalization

In this example, the effect of frequency normalization on the estimation of computational poles is presented. Using a low model order algorithm, PFD, which has a long basis, the way in which the physical frequencies are normalized from solution to solution is varied. This demonstrated that changing the frequency normalization or scaling has no effect on the true system poles; however, because of the change in frequency scaling, the spurious computational poles are estimated differently in each solution when the frequency normalization is removed. By comparing the results for different frequency scaling conditions, it becomes trivial to isolate and suppress the display of these non-structural system property artifacts.

The first plot, Figure 28, presents a traditional consistency diagram resulting from using high order coefficient normalization. It is obvious that numerous spurious computational poles are displayed. By changing to low order coefficient normalization, Figure 29, other spurious poles result. Note the quasi-stable pole just below the 370 Hz poles. Suppression of the symbols associated with the conjugate poles, Figure 30, and suppression of symbols associated with both the conjugate and consistent frequency poles, Figure 31, does not eliminate this sequence of symbols. If this were the only data being viewed, the conclusion might be drawn that there is a poorly excited mode present, just below the obvious 370 Hz modes. However, by varying the frequency normalization, Figure 32, it becomes obvious by the staggered nature of progression that this symbol sequence is merely a computational pole. Finally, the next two figures show the resultant clean consistency diagram that results by suppressing the symbols associated with the conjugate poles, Figure 33, and the symbols associated with both the conjugate and consistent frequency poles, Figure 34. A comparison of Figures 30 and 31 with Figures 33 and 34 show clearly the improved appearance of the consistency diagram through the use of varying frequency normalization.

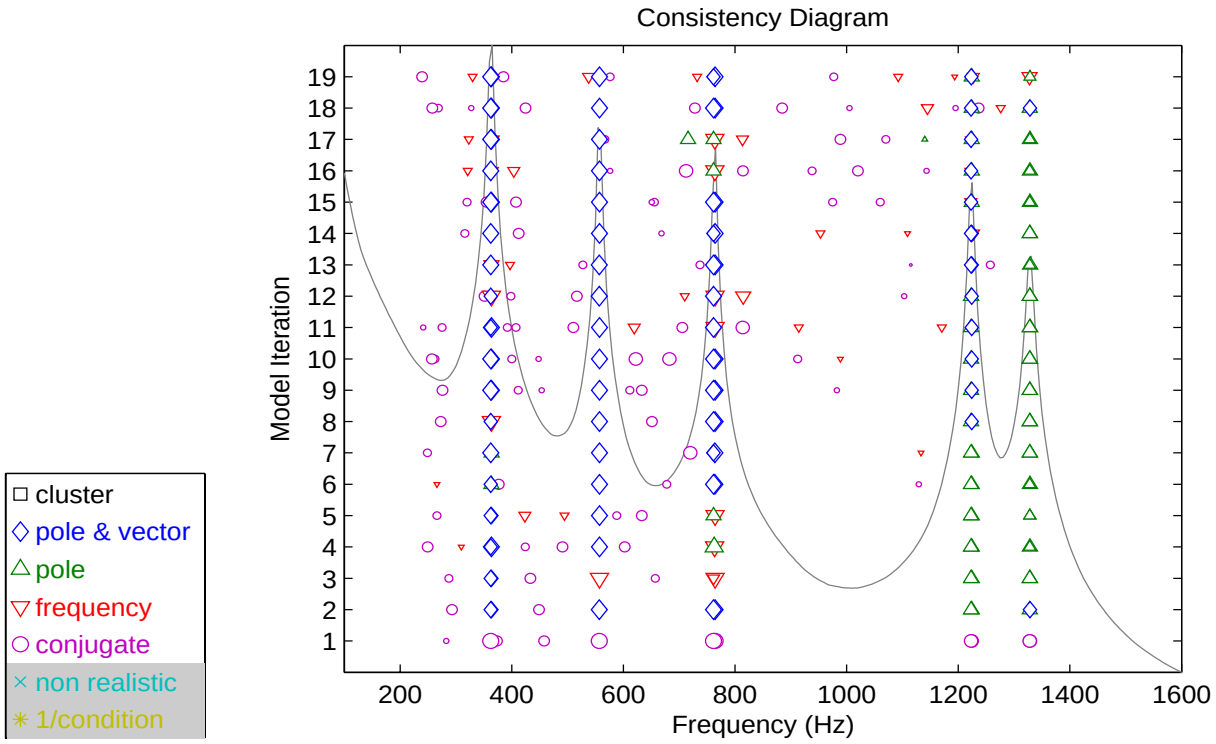

Figure 28. PFD, Long Basis, High Order Coefficient Normalization, Frequency Scaling (-2,2)

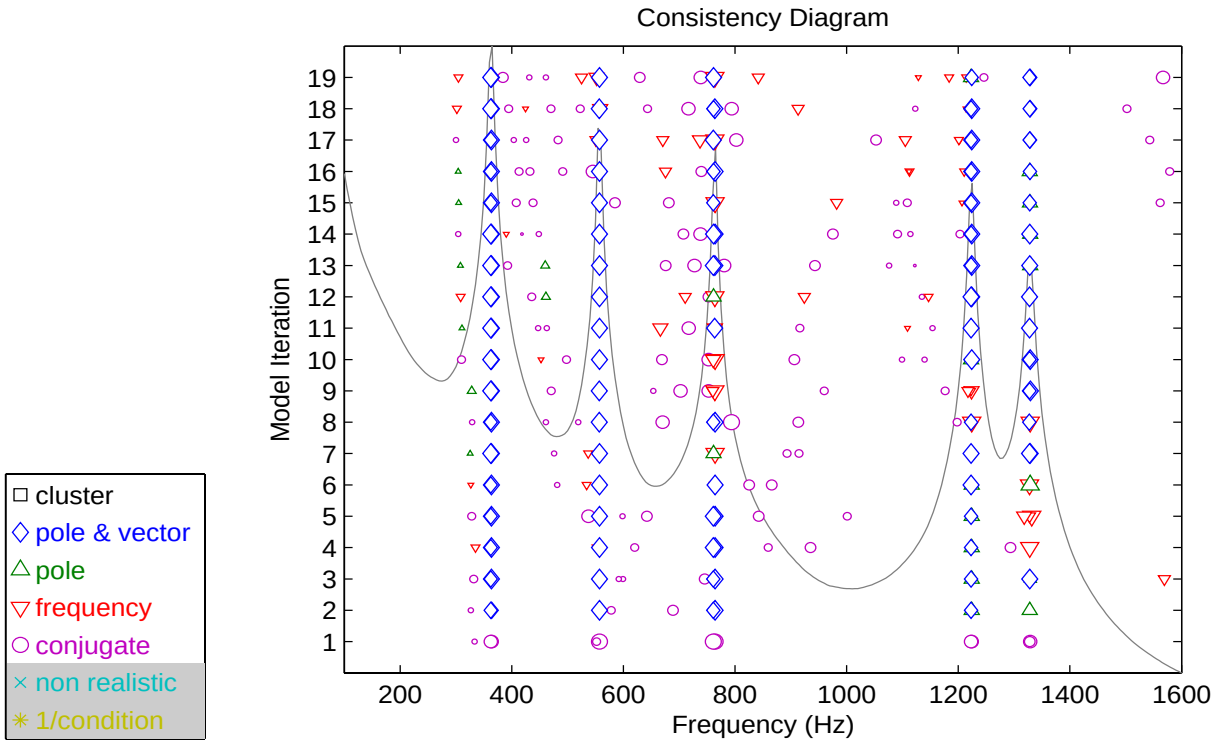

Figure 29. PFD, Long Basis, Low Order Coefficient Normalization, Frequency Scaling (-2,2)

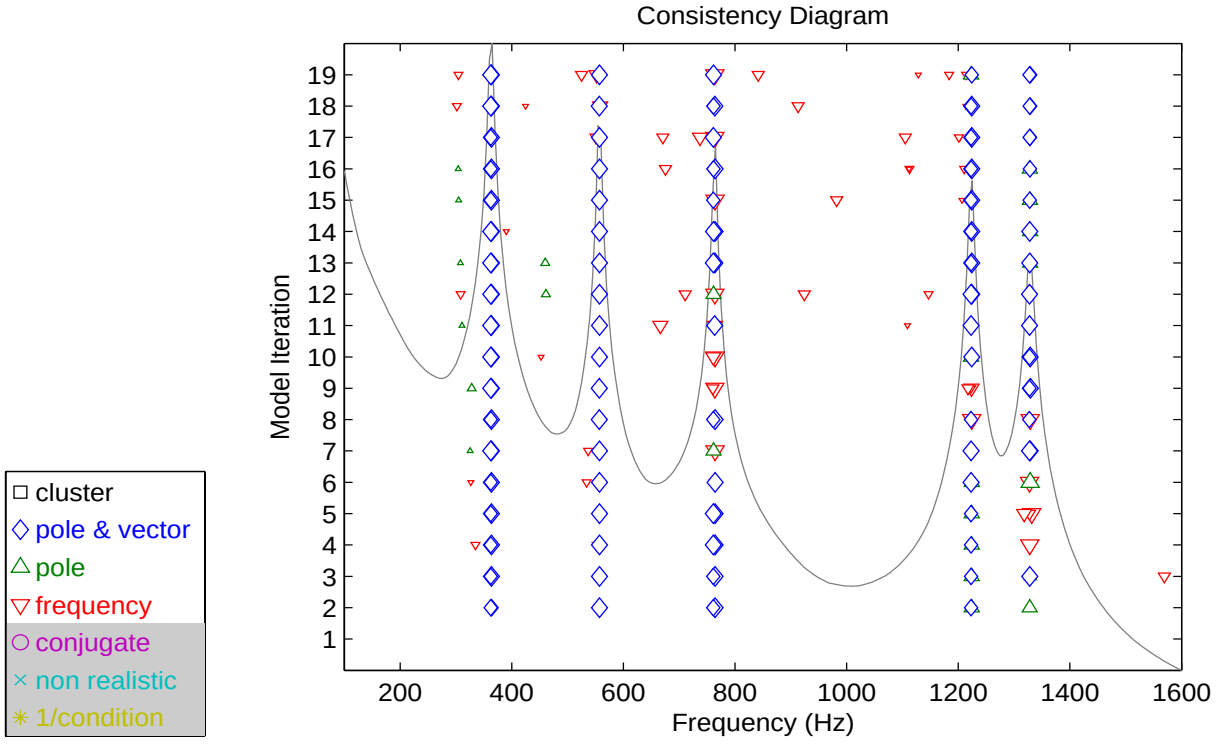

Figure 30. PFD, Long Basis, Low Order Coefficient Normalization, Frequency Scaling (-2,2), Conjugates Off

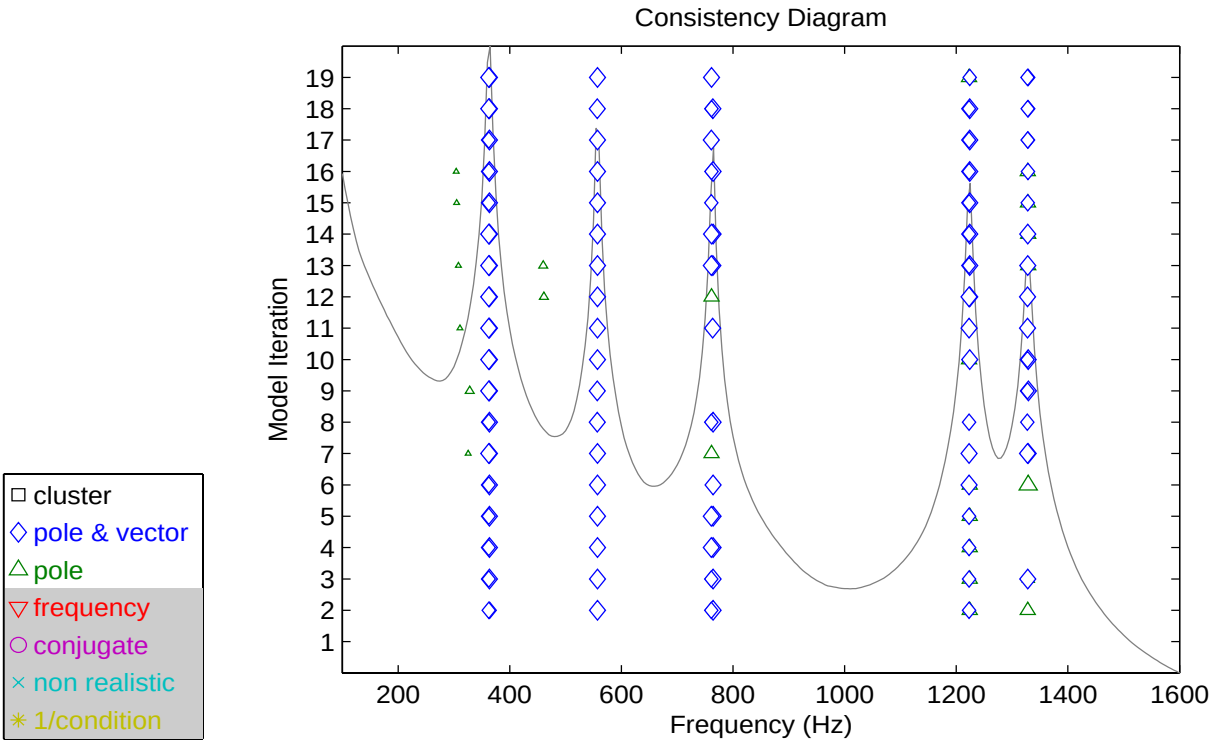

Figure 31. PFD, Long Basis, Low Order Coefficient Normalization, Frequency Scaling (-2,2), Conjugates and Frequency Off

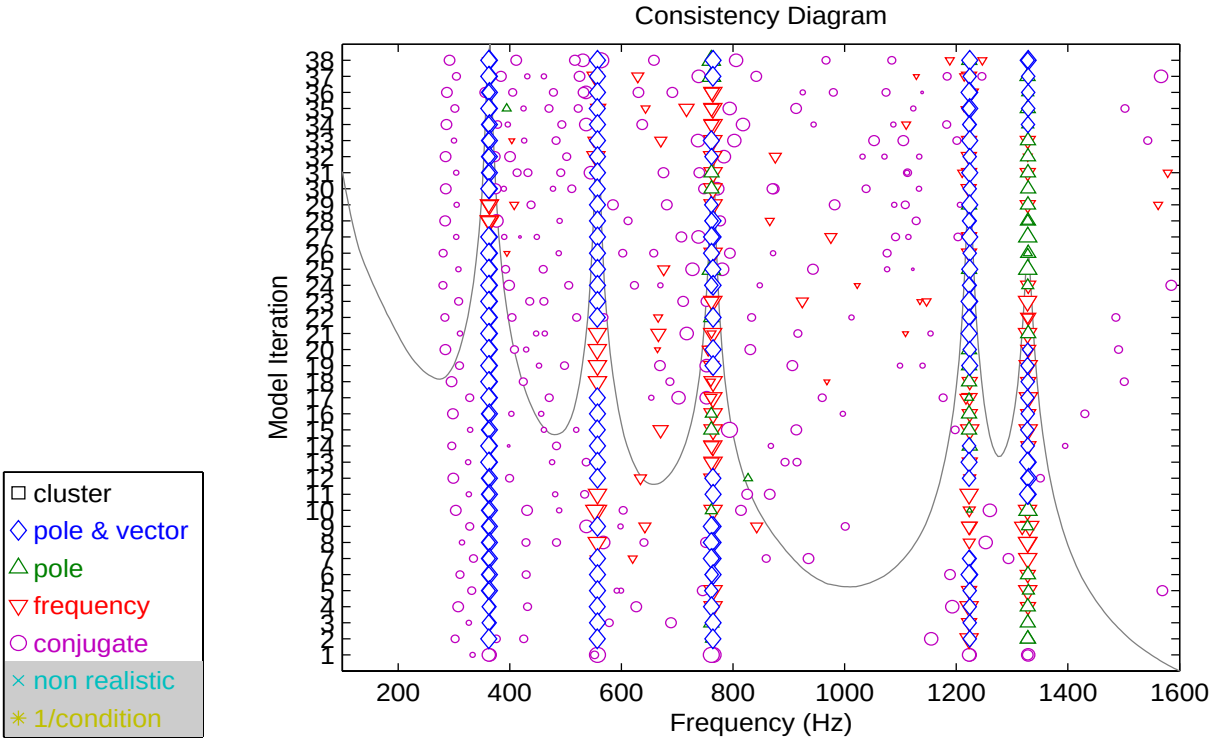

Figure 32. PFD, Long Basis, Low Order Coefficient Normalization, Alternating Frequency Scaling (-2,2)/(-1,1)

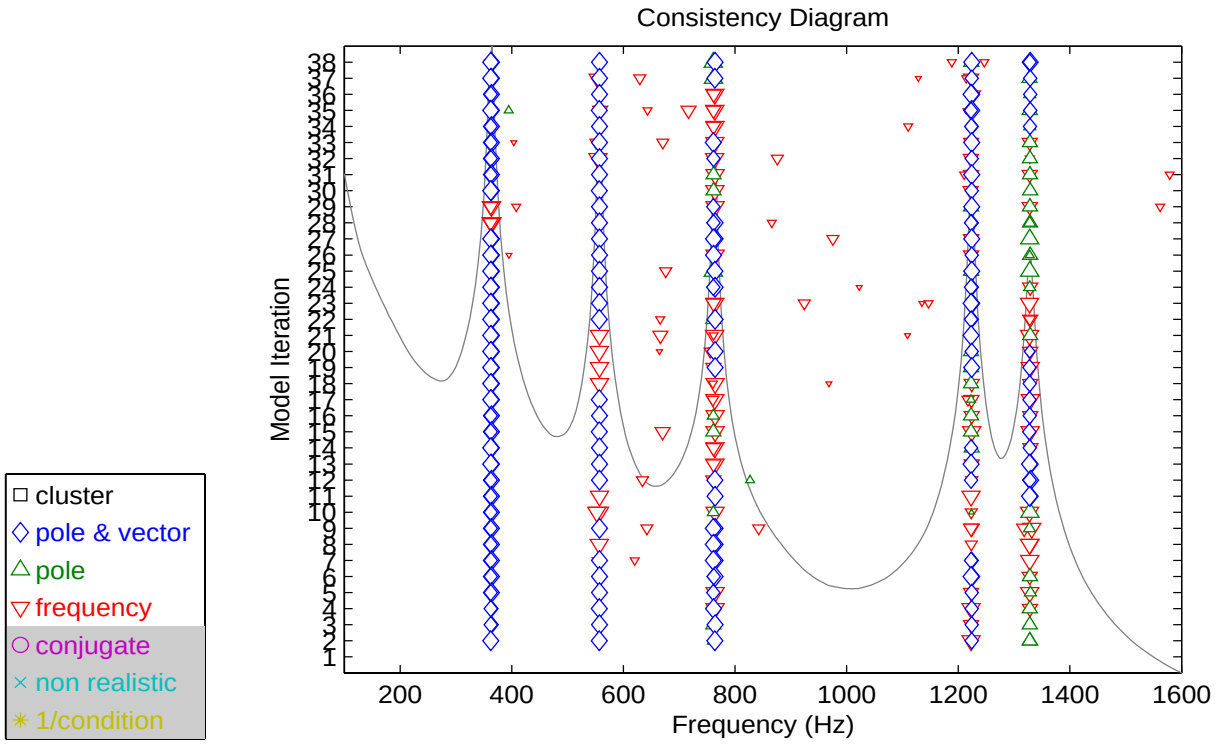

Figure 33. PFD, Long Basis, Low Order Coefficient Normalization, Alternating Frequency Scaling (-2,2)/(-1,1), Conjugates Off

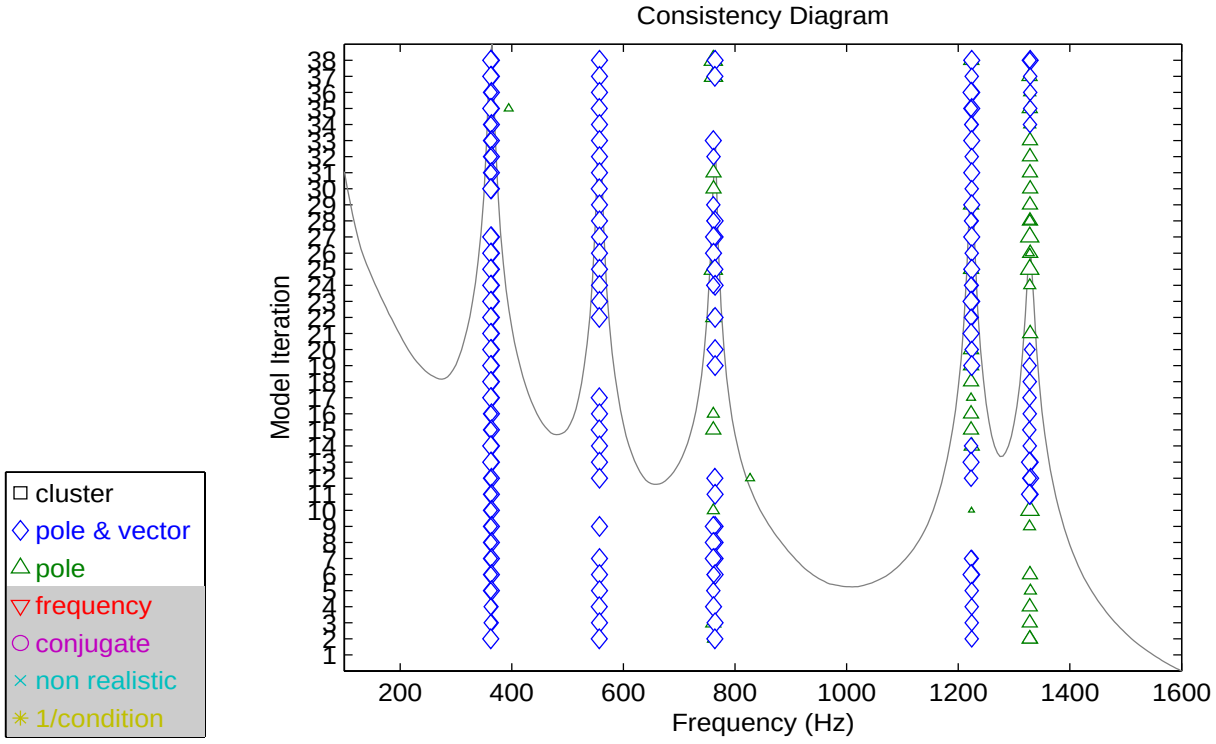

Figure 34. PFD, Long Basis, Low Order Coefficient Normalization, Frequency Scaling (-2,2)/(-1,1), Conjugates and Frequency Off

Finally, Figures 35-37 show the effect of combining several different solution method effects on the ordinate axis together with selective suppression of some of the consistency indication sysmbols. Figure 35 is the baseline case with coefficient and frequency normalization varied up the ordinate axis. Figure 36 is this same case with the symbols indicating conjugates suppressed. Figure 37 is this same case with both the conjugate and consistent frequency symbols suppressed.

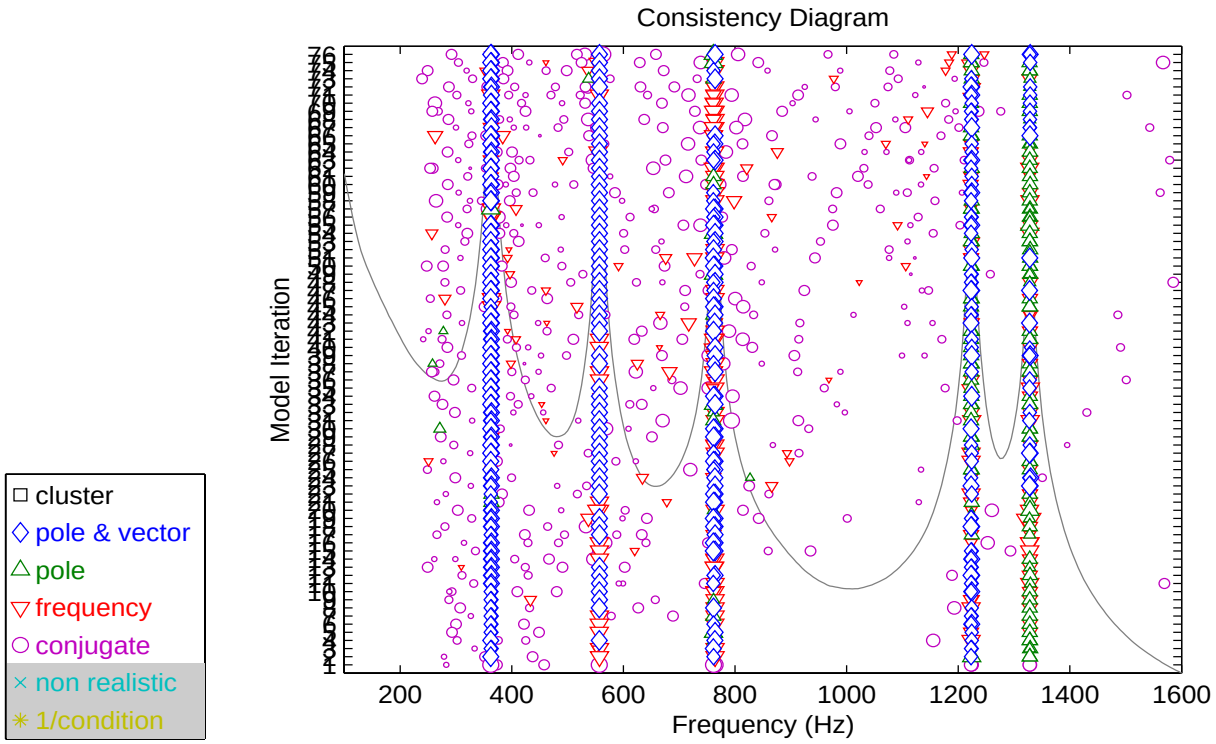

Figure 35. PFD, Long Basis, Alternating High/Low Order Coefficient Normalization, Alternating Frequency Scaling (-2,2)/(-1,1)

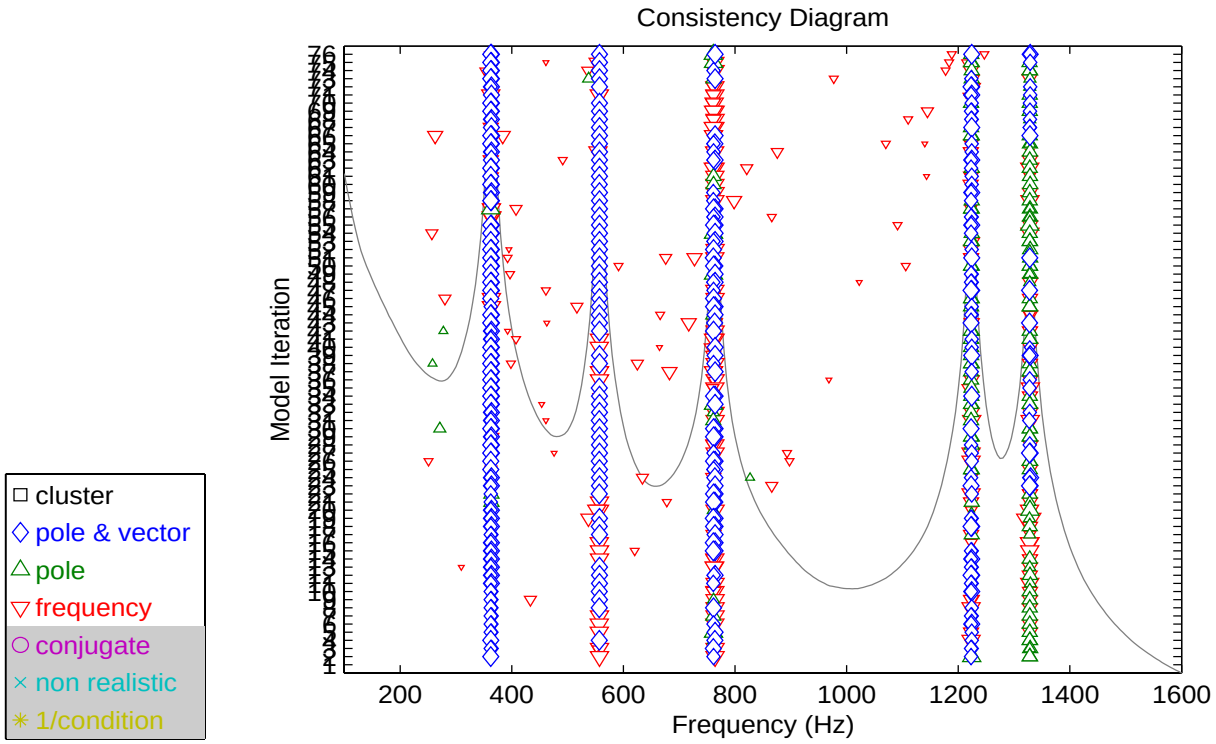

Figure 36. PFD, Long Basis, Alternating High/Low Order Coefficient Normalization, Alternating Frequency Scaling (-2,2)/(-1,1), Conjugates Off

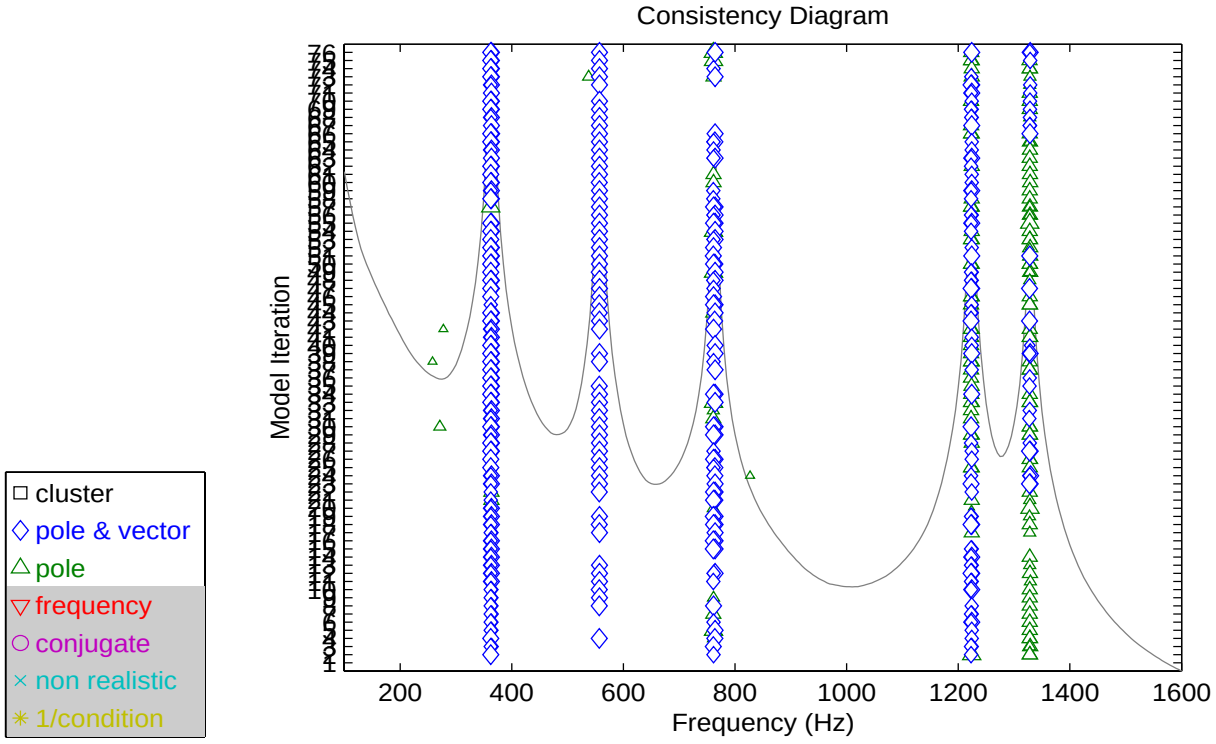

Figure 37. PFD, Long Basis, Alternating High/Low Order Coefficient Normalization, Alternating Frequency Scaling (-2,2)/(-1,1), Conjugates and Frequency Off

4. Summary

In this paper, several approaches to achieving clean, visually satisfying, user friendly and meaningful consistency diagrams have been presented. These methods have included:

- Varying the symbol size based upon normal mode criteria
- The choice to use complete or incomplete vector comparisons
- Using both high and low order coefficient normalization methods
- Varying the relationship between the numerator and denominator polynomial model order
- Fixing the denominator polynomial order and varying the numerator polynomial order
- Varying the frequency normalization used

Each of these techniques has been shown to influence the visual appearence of the consistency diagram significantly. The key in each case is the suppression of obvious artifacts between iterations thereby leaving only the most consistent solutions displayed.

The consistency diagram continues to be an effective tool for the identification of valid modal parameters. Although no single technique for organizing the ordinate axis is a universal solution, through the use of multiple techniques, any modal parameter estimation algorithm can yield clear stabilization or consistency diagrams.

5. Acknowledgements

The authors would like to acknowledge the thoughts and feedback of Mr. Charlie Pickrel of The Boeing Company for his input concerning ways to make consistency diagrams more user friendly.

6. References

[1] Brown, D.L., Allemang, R.J., Zimmerman, R.D., Mergeay, M. "Parameter Estimation Techniques for Modal Analysis", SAE Paper Number 790221, *SAE Transactions*, Volume 88, pp. 828-846, 1979.

[2] Allemang, R.J., Brown, D.L., "Summary of Technical Work", *Experimental Modal Analysis and Dynamic Component Synthesis*, USAF Technical Report, Contract Number F33615-83-C-3218, AFWAL-TR-87-3069, Volume 1, 1987.

[3] "Modal Parameter Estimation: A Unified Matrix Polynomial Approach", Allemang, R.J., Brown, D.L., Fladung, W., Proceedings, International Modal Analysis Conference, pp. 501-514, 1994.

[4] "A Unified Matrix Polynomial Approach to Modal Identification", Allemang, R.J., Brown, D.L., *Journal of Sound and Vibration*, Volume 211, Number 3, pp. 301-322, April 1998.

[5] "The Unified Matrix Polynomial Approach to Understanding Modal Parameter Estimation: An Update", Allemang, R.J., Phillips, A.W., Proceedings, International Seminar on Modal Analysis, Katholieke University of Leuven, Belgium, 36 pp., 2004.

[6] Guillaume, P., Verboven, P., Vanlanduit, S., Van der Auweraer, H., Peeters, B., "A Polyreference Implementation of the Least-Squares Complex Frequency Domain Estimator", Proceedings, International Modal Analysis Conference, 12 pp., 2003.

[7] Verboven, P., Guillaume, P., Cauberghe, B., Parloo, E., Vanlanduit, S., "Stabilization Charts and Uncertainty Bounds for Frequency Domain Linear Least Squares Estimators", Proceedings, International Modal Analysis Conference, 10 pp., 2003.

[8] Verboven, P., Cauberghe, B., Vanlanduit, S., Parloo, E., Guillaume, P., "The Secret Behind Clear Stabilization Diagrams: The Influence of the Parameter Constraint on the Stability of the Poles", Proceedings, Society of Experimental Mechanics (SEM) Annual Conference, 17 pp., 2004.

[9] Verboven, P., "Frequency Domain System Identification for Modal Analysis", PhD Dissertation, Department of Mechanical Engineering, Vrije Universiteit Brussel, Belgium, 2002.

[10] Cauberghe, B., "Application of Frequency Domain System Identification for Experimental and Operational Modal Analysis", PhD Dissertation, Department of Mechanical Engineering, Vrije Universiteit Brussel, Belgium, 259 pp., 2004.

[11] Phillips, A.W., Allemang, R.J., Pickrel, C.R., "Clustering of Modal Frequency Estimates from Different Solution Sets", Proceedings, International Modal Analysis Conference, pp. 1053-1063, 1997.

[12] "A Low Order Implementation of the Polyreference Least Squares Complex Frequency (LSCF) Algorithm", Phillips, A.W., Allemang, R.J., Proceedings, International Seminar on Modal Analysis, Katholieke University of Leuven, Belgium, 28 pp., 2004.

[13] "Data Presentation Schemes for Selection and Identification of Modal Parameters", Phillips, A.W., Allemang, R.J., Proceedings, International Modal Analysis Conference, 10 pp., 2005.

[14] Fladung, W.F., "A Generalized Residuals Model for the Unified Matrix Polynomial Approach to Frequency Domain Modal Parameter Estimation", PhD Dissertation, University of Cincinnati, 146 pp., 2001.